Chem. Rev. 1991, 91, 651-667

Approximate Density Functional Theory as a Practical Tool in Molecular Energetics and Dynamics

TOM ZIEGLER

Department of Chemistry, University of Calgary, Calgary, Alberta, Canada T2n 1N4

Received August 20, 1990 (Revised Manuscript Received February 4, 1991)

Contents

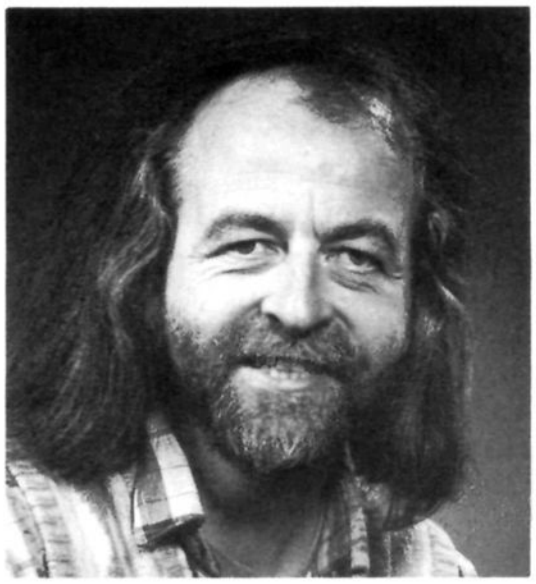

Tom Ziegler was raised in Denmark and graduated from the University of Copenhagen in 1972 with a Cand. Scient. degree in theoretical chemistry. He obtained his Ph.D. degree from University of Calgary in 1978 and is currently an associate professor at the same institution. He has been a ZWO postdoctoral fellow (1978–1980) at the Free University of Amsterdam and an NRC postdoctoral fellow (1980–1981) at McMaster University. He won an NSERC University Research Fellowship (1981–1986) which he spent at the University of Calgary. His research interest is density functional theory and its application to the structure and reactivity of transition-metal systems.

I. Introduction

Approximate density functional theory (DFT) has over the past decade emerged as a tangible and versatile computational method. It has been employed successfully to obtain thermochemical data, molecular structures, force fields and frequencies, assignments of NMR, photoelectron, ESR, and UV spectra, transition-state structures, as well as activation barriers, dipole moments, and other one-electron properties. Thus, approximate DFT is now applied to many problems previously covered exclusively by ab initio Hartree–Fock (HF) and post-HF methods. The recently acquired popularity of approximate DFT stems in large measure from its computational expedience which makes it amenable to large-size or real-life molecules at a fraction of the time required for HF or post-HF calculations. More importantly, perhaps, is the fact that expectation values derived from approximate DFT in most cases are better in line with experiment than results obtained from HF calculations. This is in particular the case for systems involving transition metals.

It is the primary objective of this review to assess the accuracy of approximate DFT by evaluating DFT results from calculations on a number of molecular properties. Emphasis will further be given to a comparison with the degree of accuracy obtained by HF and post-HF methods. Approximate DFT has over the past decade benefited immensely from a number of innovative implementations as well as the development of new and more refined approximations to DFT. These new developments will also be reviewed.

The basic notion in DFT, that the energy of an electronic system can be expressed in terms of its density, is almost as old as quantum mechanics and dates back to the early work by Thomas,[1c] Fermi,[1b] Dirac,[1a] and Wigner.[1g] The theory by Thomas and Fermi is a true density function(al) theory since all parts of the energy, kinetic as well as electrostatic, are expressed in terms of the electron density. The Thomas–Fermi method, although highly approximate, has been applied[1d-f] widely in atomic physics as a conceptually useful and computationally expedient model.

The Hartree–Fock–Slater or Xα method was one of the first DFT-based schemes to be use in studies on systems with more than one atom. The Xα theory has its origin in solid-state physics. The method emerged from the work of J. C. Slater[2a] who in 1951 proposed to represent the exchange–correlation potential by a function which is proportional to the $^1/_3$ power of the electron density. This approximation evolved out of the need to develop techniques that were able to handle solids within a reasonable time frame. DFT-based

0009-2665/91/0791-0651$09.50/0

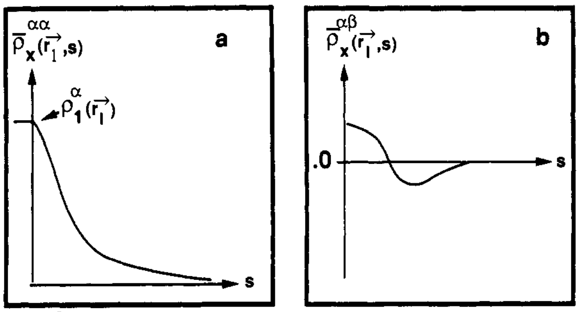

Figure 1. (a) The Fermi hole function $\bar{\rho}_x^{\alpha\alpha}(\vec{\mathbf{r}}_1, s)$ as a function of the interelectronic distance s. (b) The Coulomb hole function $\bar{\rho}_x^{\alpha\beta}(\vec{\mathbf{r}}_1, s)$ as a function of the interelectronic distance s.

methods have been predominant in solid-state physics since the pioneering work by Slater[2] and Gáspár.[2b] Slater[2d] has given a vivid account of how the Xα method evolved during the 1950's and 1960's, with reference to numerous applications up to 1974.

The Thomas–Fermi method and the Xα scheme were at the time of their inceptions considered as useful models based on the notion that the energy of an electronic system can be expressed in terms of its density. A formal proof of this notion came in 1964 when it was shown by Hohenberg[3a] and Kohn that the ground-state energy of an electronic system is uniquely defined by its density, although the exact functional dependence of the energy on density remains unknown. This important theorem has later been extended by Levy.[3b] Of further importance was the deviation by Kohn[4] and Sham of a set of one-electron equations from which one in principle could obtain the exact electron density and thus the total energy. The work of Hohenberg, Kohn, and Sham has rekindled much interest in methods where the energy is expressed in terms of the density. In particular the equations by Kohn and Sham have served as a starting point for new approximate DF methods. These schemes can now be considered as approximations to a rigorous theory rather than just models. An account of the formal developments in DFT since 1964 can be found in several important proceedings[5] and monographs[6] as well as shorter overview articles.[7] The application of DFT to solid-state physics[8] has been reviewed by a number of authors.

Quantitative quantum mechanical calculations on molecular systems have traditionally been carried out by HF or post-HF methods, with the first molecular ab initio HF-calculations dating back to the late 1950's. On the other hand, molecular calculations based on DFT did not emerge before the late 1960's. Much of the initial pioneering DFT work in chemistry has already been reviewed.[9,10] The focal point of the present account is on more recent applications of DFT to molecular systems. Thus calculations on solids and surfaces will not be covered here. Recent reviews on applications to solids[8] can be found elsewhere.

We shall begin by an overview of approximate DFT, emphasizing in particular the computational aspects as well as newer theoretical developments. The exposition will be based on the hole–correlation function which is one of the few concepts transcending the boundaries between traditional ab initio methods and DF formulations. The second part covers calculations on molecular properties with the accent on expectation values derived from energy differences. The objective here is to evaluate the accuracy of approximate DF theories for each property. We shall in particular assess the quantitative improvements one might obtain by resorting to newer and more refined approximations. It is not the intention to review all published DFT-based calculations on molecular systems, although reference will be given to a representative cross section of applications. We shall finally point to some fundamental difficulties in approximate DFT which will need to be addressed in the future.

II. General Theory

A. The Kohn–Sham Equation

The total energy of an n-electron system can be written[3] without approximations as

$$E_{\mathrm{el}} = -\tfrac{1}{2}\sum_i \int \phi_i(\vec{\mathbf{r}}_1)\nabla^2\phi_i(\vec{\mathbf{r}}_1)\,\mathrm{d}\vec{\mathbf{r}}_1 + \sum_A \int \frac{Z_A}{|\vec{\mathbf{R}}_A - \vec{\mathbf{r}}_1|}\rho(\vec{\mathbf{r}}_1)\,\mathrm{d}\vec{\mathbf{r}}_1 + \tfrac{1}{2}\int \frac{\rho(\vec{\mathbf{r}}_1)\rho(\vec{\mathbf{r}}_2)}{|\vec{\mathbf{r}}_1 - \vec{r}_2|}\,\mathrm{d}\vec{\mathbf{r}}_1\,\mathrm{d}\vec{\mathbf{r}}_2 + E_{\mathrm{xc}} \quad (1)$$

The first term in eq 1 represents the kinetic energy of n noninteracting[11] electrons with the same density $\rho(\vec{r}_1) = \sum_i\phi_i(\vec{r}_1)\phi_i(\vec{r}_2)$ as the actual system of interacting electrons. The second term accounts for the electron–nucleus attraction and the third term for the Coulomb interaction between the two charge distributions $\rho(\vec{\mathbf{r}}_1)$ and $\rho(\vec{\mathbf{r}}_2)$. The last term contains the exchange–correlation energy, E_{xc}. The exchange–correlation energy can be expressed in tems of the spherically averaged exchange–correlation hole functions[11,12,13] $\bar{\rho}_x^{\gamma\gamma'}(\vec{\mathbf{r}}_1, s)$ as

$$E_{\mathrm{XC}} = \sum_{\gamma}\sum_{\gamma'} -4\pi/2 \int \frac{\rho_1^{\gamma}(\vec{\mathbf{r}}_1)\bar{\rho}_x^{\gamma\gamma'}(\vec{\mathbf{r}}_1, s)}{s}\,\mathrm{d}\vec{\mathbf{r}}_1 s^2\,\mathrm{d}s \quad (2)$$

where the spin indices γ and γ' both run over α-spin as well as β-spin and $s = |\vec{\mathbf{r}}_1 - \vec{\mathbf{r}}_2|$.

The one-electron orbitals, $\{\phi_i(\vec{\mathbf{r}}_1); i = 1, n\}$, of eq 1 are solutions to the set of one-electron Kohn–Sham equations[4]

$$\left[-\tfrac{1}{2}\nabla^2 + \sum_A \frac{Z_A}{|\vec{\mathbf{R}}_A - \vec{\mathbf{r}}_1|} + \int \frac{\rho(\vec{\mathbf{r}}_2)}{|\vec{\mathbf{r}}_1 - \vec{\mathbf{r}}_2|}\,\mathrm{d}\vec{\mathbf{r}}_2 + V_{\mathrm{XC}}\right]\phi_i(\vec{\mathbf{r}}_1) = h_{\mathrm{KS}}\,\phi_i(\vec{\mathbf{r}}_1) = \epsilon_i\phi_i(\vec{\mathbf{r}}_1) \quad (3)$$

where the exchange–correlation potential V_{XC} is given as the functional derivative of E_{XC} with respect to the density[4]

$$V_{\mathrm{XC}}[\rho] = \delta E_{\mathrm{XC}}[\rho]/\delta\rho \quad (4)$$

The hole function $\bar{\rho}_x^{\gamma\gamma'}(\vec{\mathbf{r}}, s)$ contains all information about exchange and correlation between the interacting electrons as well as the influence[11b] of correlation on the kinetic energy. The interpretation of $\bar{\rho}_x^{\gamma\gamma'}(\vec{\mathbf{r}}_1, s)$ is that an electron at $\vec{\mathbf{r}}_1$ to a larger or smaller extent will exclude other electrons from approaching within a distance s. The extent of exclusion or screening increases with the magnitude of $\bar{\rho}_x^{\gamma\gamma'}(\vec{\mathbf{r}}_1, s)$. Examples of the hole function are shown in Figure 1 for $\gamma = \gamma'$, part a, as well as $\gamma \neq \gamma'$, part b. The intricate function, $\bar{\rho}_x^{\gamma\gamma'}(\vec{\mathbf{r}}_1, s)$, can in practice[14] only be obtained from an exact solution to the Schrödinger equation of our n-electron system. The set of one-electron Kohn–Sham equations is as a consequence of limited value for exact[14] solutions to many-electron systems. They form, however, the starting point for an approximate treatment in which $\bar{\rho}_{\mathrm{x}}^{\gamma\gamma'}(\vec{\mathbf{r}}_1, s)$ is replaced by model hole functions. The form of the exact hole function $\bar{\rho}_{\mathrm{x}}^{\gamma\gamma'}(\vec{\mathbf{r}}_1, s)$ is not known in detail. Nevertheless, a number of properties of $\bar{\rho}_{\mathrm{x}}^{\gamma\gamma'}(\vec{\mathbf{r}}_1, s)$ can be deduced from general considerations.[12,13] Thus, it is readily shown[13] that the spherically averaged (Coulomb) hole–correlation functions, $\bar{\rho}_{\mathrm{x}}^{\gamma\gamma'}(\vec{\mathbf{r}}_1, s)$, with $\gamma \neq \gamma'$, have the following properties

$$4\pi \int \bar{\rho}_{\mathrm{x}}^{\gamma\gamma'}(\vec{\mathbf{r}}_1, s) s^2 \, \mathrm{d}s = 0 \tag{5a}$$

whereas the corresponding (Fermi) functions $\bar{\rho}_{\mathrm{x}}^{\gamma\gamma}(\vec{\mathbf{r}}_1, s)$, with $\gamma = \gamma'$, satisfy the normalization condition

$$4\pi \int \bar{\rho}_{\mathrm{x}}^{\gamma\gamma'}(\vec{\mathbf{r}}_1, s) s^2 \, \mathrm{d}s = 1 \tag{5b}$$

Further, for the Fermi contributions

$$\bar{\rho}_{\mathrm{x}}^{\gamma\gamma}(\vec{\mathbf{r}}_1, 0) = \rho_1^{\gamma}(\vec{\mathbf{r}}_1) \tag{5c}$$

The two Coulomb functions $\bar{\rho}_{\mathrm{x}}^{\alpha\beta}(\vec{\mathbf{r}}_1, 0)$ and $\bar{\rho}_{\mathrm{x}}^{\beta\alpha}(\vec{\mathbf{r}}_1, 0)$ are in general considered to be smaller than $\bar{\rho}_{\mathrm{x}}^{\gamma\gamma}(\vec{\mathbf{r}}_1, 0)$, although different from zero. They cannot be related to $\rho_1^{\gamma}(\vec{\mathbf{r}}_1)$ in a simple way.

The model hole functions are in general[6a] constructed in such a way that the constraints given in eqs 5a–c are satisfied. Thus, the Fermi function of Figure 1a with $\gamma = \gamma'$ is seen to satisfy the constraints of eqs 5b,c, whereas the Coulomb function of Figure 1b with $\gamma \neq \gamma'$ satisfies eq 5a. We shall in the following briefly review some of the models that have found more extensive applications in electronic structure calculations on atoms and molecules.

B. Local Density Approximations

The homogeneous electron gas has been particularly instrumental[13b,15] in fostering useful approximate expressions for the exchange–correlation energy. The exchange–correlation energy for the homogeneous electron gas can be written as

$$E_{\mathrm{XC}}^{\mathrm{LDA}} = E_{\mathrm{X}}^{\mathrm{LDA}} + E_{\mathrm{C}}^{\mathrm{LDA}} \tag{6}$$

The first term, representing the exchange energy, has the form

$$E_{\mathrm{X}}^{\mathrm{LDA}} = -9/4\alpha_{\mathrm{ex}}[3/4\pi]^{1/3} \sum_{\gamma} \int [\rho_1^{\gamma}(\vec{\mathbf{r}}_1)]^{4/3} \, \mathrm{d}\vec{\mathbf{r}}_1 \tag{7}$$

where the electron gas value for the exchange scale factor α_{ex} is $^2/_3$. The exact exchange energy in the Kohn–Sham theory is simply E_{xc} corresponding to a single determinantal wave function constructed from the exact Kohn–Sham orbitals. The second term, representing the correlation energy, has the form

$$E_{\mathrm{C}}^{\mathrm{LDA}} = \int \rho_1(\vec{\mathbf{r}}_1) \epsilon_{\mathrm{c}}[\rho_1^{\alpha}(\vec{\mathbf{r}}_1)\ \rho_1^{\beta}(\vec{\mathbf{r}}_1)] \, \mathrm{d}\vec{\mathbf{r}}_1 \tag{8}$$

where $\epsilon_{\mathrm{c}}[\rho_1^{\alpha},\rho_1^{\beta}]$ represents the correlation energy per electron in a gas with the spin densities ρ_1^{α} and ρ_1^{β}. The specific correlation energy, $\epsilon_{\mathrm{c}}[\rho_1^{\alpha},\rho_1^{\beta}]$, is not known analytically. However, approximations[13b,15] of increasing accuracy have been developed. Most recently[16] Vosko, Wilk, and Nusair have used Padé interpolations to fit $\epsilon_{\mathrm{c}}[\rho_1^{\alpha},\rho_1^{\beta}]$ from accurate calculation on the homogeneous electron gas due to Ceperley[17] and Alder. The representation of the exchange–correlation energy by eq 6 has been coined[13b] the local density approximation (LDA).

TABLE I. Atomic Exchange Energies (au)

	exact[a]	LDA[b]	GC[c]	Becke[d]	Kress[e]	TZ[f]
He	−1.026	−0.884	−1.074	−1.025	−1.023	−1.017
Ne	−12.11	−11.03	−12.18	−12.14	−12.14	−12.14
Ar	−30.19	−27.86	−30.08	−30.15	−30.16	−30.19
Kr	−93.89	−88.62	−93.32	−93.87	−93.81	−93.97
Xe	−179.2	−170.6	−177.9	−179.0	−178.8	−179.1

[a] From HF calculations. [b] From LDA calculations using eq 7 with $\alpha_{\mathrm{ex}} = {}^2/_3$. [c] Using eq 9 with $g(\chi^{\gamma})$ given by ref 20. [d] Using eq 9 with $g(\chi^{\gamma})$ given by ref 23d. [e] Using eq 9 with $g(\chi^{\gamma})$ given by ref 23e. [f] Using eq 9 with $g(\chi^{\gamma})$ given by ref 19.

TABLE II. Errors[a] in Correlation Energies Determined from Various Density Functional Methods (au)

	exact	LDA[a]	CS[a,b]	SPP[a,c]	PD[a,d]	B[a,e]
He	0.0420	0.07	−0.0004	0.017	0.003	0.000
Be	0.094	0.131	−0.0014	0.022	0.001	−0.002
C	0.156	0.203	0.005	0.020	0.009	0.007
N	0.189	0.241	0.001	0.015	0.017	0.013
Ne	0.387	0.359	0.012	−0.001	0.008	0.001

[a] The difference is given by $E_{\mathrm{c}}^{\mathrm{exp}} - E_{\mathrm{c}}^{\mathrm{cal}}$. [b] Reference 26b. [c] Reference 24. [d] Reference 25. [e] Reference 11.

Simplified versions of LDA were known[1] long before the formal development of DFT. Of particular importance is the Hartree–Fock–Slater, or Xα, method developed by Slater[3] and others.[18] This method retains only the exchange part (see eq 7) of the total expression for the exchange–correlation energy given in eq 6 and adopts in many cases values for the exchange scaling factor that differs[13a,b] somewhat from $^2/_3$.

The exchange–correlation hole functions for the homogeneous electron gas satisfy the general constrains given in eq 5 and can thus be used as models for calculations on atoms and molecules by substituting the corresponding (inhomogeneous) electron densities into the expression for the exchange–correlation energy in eq 6. Table I compares, for the noble gas atoms, the exchange energy calculated by the LDA method according to eq 7 ($\alpha_{\mathrm{ex}} = {}^2/_3$) with the exact exchange energy from Hartree–Fock (HF) calculations. The LDA values are seen to be between 3–10% too small which in absolute terms amounts to more than 10^5 kJ/mol (!) for Xe.

Table II compares, again for a number of atoms, correlation energies calculated by LDA according to eq 7 with experiment. The LDA is seen to overestimate correlation energies by 100%. However, the correlation error is smaller in absolute terms then the corresponding exchange error. We shall in the next section discuss ways in which one might improve upon the LDA expression for the exchange–correlation energy.

C. Nonlocal Extensions to LDA

The exchange part of the Fermi hole function for the homogeneous electron gas is given by

$$\bar{\rho}_{\mathrm{X}\alpha}^{\gamma\gamma}(\vec{\mathbf{r}}_1, s) = \rho_1^{\gamma}(\vec{\mathbf{r}}_1) \cdot 9[[\sin(k_{\mathrm{f}}s) - k_{\mathrm{f}}s \cdot \cos(k_{\mathrm{f}}s)]^2/(k_{\mathrm{f}}s)^6] \tag{9}$$

where $k_{\mathrm{f}} = [6\pi^2 \rho_1^{\gamma}(\vec{\mathbf{r}}_1)]^{1/3}$; $\gamma = \alpha, \beta$. It is characteristic for the exchange hole function of the homogeneous electron gas (Figure 2) that it has its principle maximum

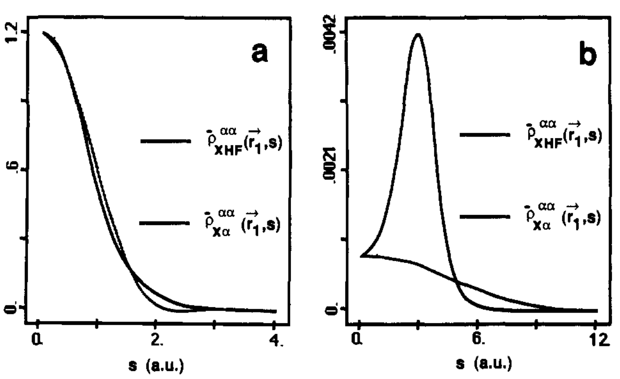

Figure 2. Spherically averaged hole correlation functions $\bar{\rho}^{\gamma\gamma}_{\text{xHF}}(\vec{\mathbf{r}}_1, s)$ and $\bar{\rho}^{\gamma\gamma}_{\text{x}\alpha}(\vec{\mathbf{r}}_1, s)$ for the HF and HFS methods, respectively. Here s is the interelectronic distance and $_1$ is the distance of the reference electron from the nuclei. (a) Hydrogen atom with $\mathbf{r}_1 = 0.5$ au. (b) Hydrogen atom with $\mathbf{r}_1 = 3.0$ au.

at $s = 0$ for all positions, $\vec{\mathbf{r}}_1$, of the reference electron. Thus, the maximum exclusion or screening is always near the reference electron. This is also the case for the exact exchange hole, $\bar{\rho}^{\gamma\gamma}_{\text{xHF}}(\vec{\mathbf{r}}_1, s)$, in molecules and atoms (see Figure 2a) with the notable exceptions[19] where $\vec{\mathbf{r}}_1$ is positioned at the border between two core shells or in the exponential tail of the valence density. For the latter two cases the function $\bar{\rho}^{\gamma\gamma}_{\text{xHF}}(\vec{\mathbf{r}}_1, s)$ has, for clear physical reasons,[19] its maximum at larger values of s as shown in Figure 2b. Thus, $\bar{\rho}^{\gamma\gamma}_{\text{x}\alpha}(\vec{\mathbf{r}}_1, s)$ has in those cases a qualitative incorrect behavior.

It is possible, as shown by Becke[20] and others,[19,21] to model the exchange hole function in such a way that it has the correct qualitative behavior for all positions of $\vec{\mathbf{r}}_1$ in finite systems. The corresponding exchange-energy expression is given by

$$\tilde{E}_{\text{x}} = E_{\text{X}}^{\text{LDA}} + E_{\text{X}}^{\text{NL}} \tag{10}$$

where the so-called nonlocal correction E_{X}^{NL} takes the form

$$E_{\text{X}}^{\text{NL}} = \sum_{\gamma} \int g(\chi^{\gamma})[\rho_1^{\gamma}(\vec{\mathbf{r}}_1)]^{4/3}\,d\vec{\mathbf{r}}_1 \tag{11a}$$

with $g(\chi^{\gamma})$ being a function of the dimensionless parameter

$$\chi^{\gamma} = |\nabla\rho_1^{\gamma}(\vec{\mathbf{r}}_1)|/[\rho_1^{\gamma}(\vec{\mathbf{r}}_1)]^{4/3} \tag{11b}$$

The expression for E^{X}_{NL} can also be derived from dimensional arguments.[22] It contains the gradient of $\rho_1^{\gamma}(\vec{\mathbf{r}}_1)$ which clearly is a measure for the inhomogeneity of the electron density in finite systems. It is for this reason often referred to as the inhomogeneous gradient correction to $E_{\text{X}}^{\text{LDA}}$. A number of different functional forms for $g(\chi^{\gamma})$ have been proposed.[23] Table I displays atomic exchange energies calculated according to eq 9 for various forms of $g(\chi^{\gamma})$. The inclusion of the nonlocal correction, E_{X}^{NL}, is seen to bring the calculated exchange energies in line with the exact values within 0.2 au. The recent form for $g(\chi^{\gamma})$ suggested by Becke[23d] is of particular interest since it has the correct asymptotic behavior for $\vec{\mathbf{r}}_1$ positioned in the exponential tail of the valence density.

The LDA overestimates, as illustrated in Table II, the correlation energies by 100%. Stoll[24] et al. have shown that the major part of the error comes from correlation between electrons of the same spin, which in finite systems is much smaller than in the homogeneous electron gas. They suggested to replace $E_{\text{C}}^{\text{LDA}}$ of eq 8 by

SCHEME I

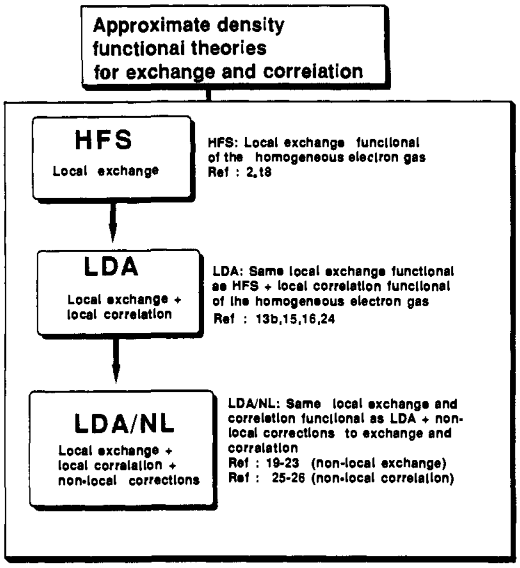

$$E_{\text{C}}^{\text{SPP}} = \int \rho_1(\vec{\mathbf{r}}_1)\epsilon_{\text{c}}[\rho_1^{\alpha}(\vec{\mathbf{r}}_1), \rho_1^{\beta}(\vec{\mathbf{r}}_1)]\,d\vec{\mathbf{r}}_1 - \int \rho_1^{\beta}(\vec{\mathbf{r}}_1)\epsilon_{\text{c}}[0, \rho_1^{\beta}(\vec{\mathbf{r}}_1)]\,d\vec{\mathbf{r}}_1 - \int \rho_1^{\alpha}(\vec{\mathbf{r}}_1)\epsilon_{\text{c}}[\rho_1^{\alpha}(\vec{\mathbf{r}}_1), 0]\,d\vec{\mathbf{r}}_1 \tag{12}$$

in which correlation between electrons of the same spin has been eliminated altogether so that contribution to the exchange–correlation energy from electrons of the same spin is given solely by the exchange part. The correlation energies calculated by $E_{\text{C}}^{\text{SPP}}$ is seen to be in error by less than 10% (Table II). The shortcomings of $E_{\text{C}}^{\text{LDA}}$ has alternatively been dealt with by considering inhomogeneous gradient corrections,[23b,25] in analogy to the exchange energy, as well as specific shapes[11b,26] and constrains[26c,6e] of the Coulomb hole function $\bar{\rho}_{\text{x}}^{\alpha\beta}(\vec{\mathbf{r}}_1, s)$. The accuracy of these correlation–energy functional are impressive as indicated in Table II. Savin[27] et al. as well as Clementi[33,34] et al. have assessed some of the proposed correlation density functions in molecular calculations. The different approximate DF theories for exchange and correlation are summarized in Scheme I.

D. Approximate Density Functional Approaches with Exact Exchange

It would seem that one could eliminate the predominant error in the LDA approach by simply calculating the exchange part exactly using the Hartree–Fock method. In this case the exchange–correlation energy is given by

$$E_{\text{XC}}^{\text{HF-LDA}} = E_{\text{X}}^{\text{HF}} + E_{\text{C}}^{\text{LDA}} \tag{13}$$

This expression has some merits for atoms,[28] but it is in fact rather inadequate for molecules.[29,30]

The HF method lacks by definition correlation, and in molecules, one has to add two types of correlation contributions to E_{X}^{HF} in order to obtain an adequate exchange–correlation energy. The first type describes the correlated movement of electrons at short interelectronic distances. It is often referred to as dynamic correlation.[31] This type of correlation is well represented[29] by $E_{\text{C}}^{\text{LDA}}$. The second category, called near

SCHEME II

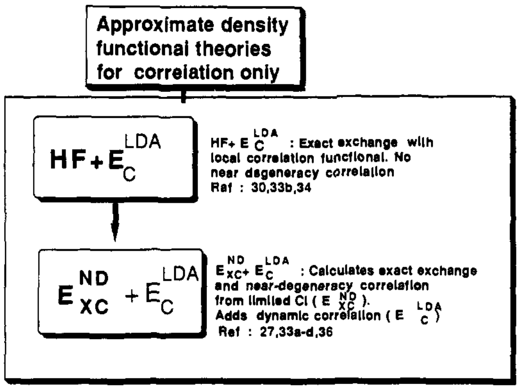

degeneracy correlation,[31] is largely a correction to E_X^{HF}. This correction is required since the molecular HF hole function, $\bar{\rho}_{XHF}^{\gamma\gamma}(\vec{r}_1, s)$, is too diffuse[29b] as a function of the interelectronic distance s for certain positions of $\vec{r}_1$, in particular in the limit of bond dissociation.[32] Thus near degeneracy correlation has largely the effect of compacting the total hole-correlation function. The term E_C^{LDA} does not contain near degeneracy correlation.[11] Molecular calculations based on eq 13 have as a consequent many of the deficiencies exhibited by the HF method. In fact, calculated bond energies based on eq 13 differ[30] in many cases considerably from experimental values.

The hole function, $\bar{\rho}_{X\alpha}^{\gamma\gamma}(\vec{r}_1, s)$, of (eq 9) does not suffer[29b] from the same deficiencies as $\bar{\rho}_{XHF}^{\gamma\gamma}(\vec{r}_1, s)$ for large s. It is thus not necessary to apply near degeneracy corrections to E_X^{LDA} of eq 7 and this is also the case[29c] if use is made of the gradient-corrected exchange energy, $\tilde{E}_x$, of eq 10. Molecular calculations in which both exchange and correlation are treated by LDA afford[30] for this reason better bond energies and bond distances than calculations based on E_{XC}^{HF-LDA}. We shall illustrate this point further in section III.

Several authors[33,34] have attempted to overcome the inadequacies of E_{XC}^{HF-LDA} by evaluating the exchange energy and the near degeneracy correlation energy as the total exchange-correlation energy, E_{XC}^{ND}, from a proper dissociation wave function.[35] The total exchange-correlation energy, E_{XC}^{ND-LDA}, is thus obtained by adding E_C^{LDA} according to

$$E_{XC}^{ND-LDA} = E_{XC}^{ND} + E_C^{LDA} \tag{14}$$

This is a very promising,[36] if somewhat involved, approach. The theoretical justification for combining E_{XC}^{ND} and E_C^{LDA} has been assessed recently by Savin.[36] A summary of the different density functional methods in which exchange is evaluated exactly is given in Scheme II.

E. Practical Implementations

The self-consistent (SCF) version of DFT, as formulated by Kohn and Sham,[4] necessitates the solution of the Kohn-Sham equation given in eq 3. This is accomplished in practice by deriving the potential V_{XC} from an approximate expression, $\tilde{E}_{XC}$, for the exact exchange-correlation energy, E_{XC}. The corresponding approximate Kohn and Sham equation reads

$$[-\tfrac{1}{2}\nabla^2 + V_N(\vec{r}_1) + V_C(\vec{r}_1) + \tilde{V}_{XC}(\vec{r}_1)]\phi_i(\vec{r}_1) = \hat{h}_{KS}\phi_i(\vec{r}_1) = \epsilon_i\phi_i(\vec{r}_1) \tag{15a}$$

where

$$V_N(\vec{r}_1) = \sum_A \frac{Z_A}{|\vec{R}_A - \vec{r}_1|} \tag{15b}$$

and

$$V_C(\vec{r}_1) = \int \frac{\rho(\vec{r}_2)}{|\vec{r}_1 - \vec{r}_2|}\, d\vec{r}_2 \tag{15c}$$

whereas

$$\tilde{V}_{XC}[\rho(\vec{r}_1)] = [\delta E_{XC}[\rho(\vec{r}_1)]]/[\delta\rho(\vec{r}_1)] \tag{15d}$$

The set of solutions, $\{\phi_i(\vec{r}_1), i = 1, n\}$, to eq 15a affords the electron density from which several expectation values can be evaluated, including the total energy.

It is customary in practical implementations to expand $\phi_i(\vec{r}_1)$ in terms of a known (basis) set of functions, $\{\chi_k(\vec{r}_1), k = 1\ M\}$, as

$$\phi_i(\vec{r}_1) = \sum_{k=1}^{k=M} C_{ik}\chi_k(\vec{r}_1) \tag{16}$$

The problem of solving the differential equation of eq 15a is now transformed into finding a set of eigenvectors $\{C_{ik}, k = 1, n; k = 1,M\}$ and corresponding eigenfunctions from the secular equation

$$\sum_{\mu=1}^{\mu=M} [F_{\nu\mu} - \epsilon_i S_{\nu\mu}] = 0,\ \nu = 1, M \tag{17a}$$

with

$$F_{\nu\mu} = \int \chi_\nu(\vec{r}_1)\hat{h}_{KS}\chi_\mu(\vec{r}_1)\, d\vec{r}_1 \tag{17b}$$

and

$$S_{\nu\mu} = \int \chi_\nu(\vec{r}_1)\chi_\mu(\vec{r}_1)\, d\vec{r}_1 \tag{17c}$$

In the earliest implementation applied to molecular problems, Johnson[37] used scattered-plane waves[38] as a basis, and the exchange-correlation energy was represented by eq 7. This SW-Xα method employed in addition an (muffin-tin) approximation[37] to the Coulomb potential of eq 15c according to which $V_C(\vec{r}_1)$ is replaced by a sum of spherical potentials around each atom. This approximation is well suited for solids for which the SW-Xα method[38] originally was developed. However, it is less appropriate in molecules where the potential around each atom might be far from spherical. The SW-Xα method is computationally expedient compared to standard ab initio techniques and has been used with considerable success[10] to elucidate the electronic structure in complexes and clusters of transition metals. However, the use of the muffin-tin approximation precludes accurate calculations of total energies. The method has for this reason not been successful[39] in studies involving molecular structures and bond energies.

The first implementations of self-consistent DFT, without recourse to the muffin-tin approximations, are due to Ellis and Painter,[40] Baerends[41] et al., Sambe and Felton,[42] Dunlap[43] et al., as well as Gunnarson[44] et al. Other implementations[45] and refinements have also appeared more recently. The accurate representation of $V_C(\vec{r}_1)$ is in general accomplished by fitting the molecular density to a set of one-center auxiliary functions[41,43,45a,46c] $f_\eta(\vec{r}_1)$, as

$$\tilde{\rho}(\vec{r}_1) \approx \sum_{\eta} a_{\eta} f_{\eta}(\vec{r}_1) \tag{18}$$

from which $V_C(\vec{r}_1)$ can now be evaluated expediently by analytical[41] or numerical[46c] integration as

$$\tilde{V}_C(\vec{r}_1) \approx \sum_{\eta} a_{\eta} \int \frac{f_{\eta}(\vec{r}_2)}{|\vec{r}_1 - \vec{r}_2|} d\vec{r}_2 \tag{19}$$

The matrix elements $F_{\nu\mu}$ and $S_{\nu\mu}$ can subsequently be obtained from numerical integration[40,46] as

$$F_{\nu\mu} = \sum_{k} \chi_{\nu}(\vec{r}_k) \tilde{h}_{KS} \chi_{\mu}(\vec{r}_k) W(\vec{r}_k) \tag{20}$$

where $W(\vec{r}_k)$ is a weight factor.[40,46] The extensive use of numerical integration is amiable to modern vector machines.[47,48] However, care must be exercised in order to calculate total energies accurately. This requirement has been met by the development of special algorithms[45a,49] as well as new accurate integration schemes.[46] The adaptation of procedures based on numerical integration techniques makes it easy to deal even with complicated expressions for the potential, $\tilde{V}_{XC}(\vec{r}_1)$. The often intricate form of the potential $\tilde{V}_{XC}(\vec{r}_1)$ precludes on the other hand a direct analytical evaluation of $F_{\nu\mu}$. However, this problem can be side-stepped by fitting[43] $\tilde{V}_{XC}(\vec{r}_1)$ to a set of auxiliary functions such as

$$\tilde{V}_{XC}(\vec{r}_1) \approx \sum_{\eta} b_{\eta} g_{\eta}(\vec{r}_1) \tag{21}$$

with the help of numerical integration techniques.[43] A substitution of eq 21 and eq 19 into eq 17a now allows for an analytical evaluation[43,48] of $F_{\nu\mu}$. The analytical procedure has the merit that advantage can be made of techniques already employed in ab initio methods. It also ensures accurate total energies in a relatively straightforward way. However, the price one must pay is the introduction of several sets of auxiliary functions.

A unique approach has lately been taken by Becke[50] in which eq 15a is solved directly without basis sets. This approach, which seems promising, was first applied to diatomic molecules[50a,b] and more recently to polyatomics.[50c–e] Alternative schemes have recently been proposed for diatomics.[51]

The various SCF schemes based on DFT are attractive alternatives to conventional ab initio methods in studies on large-size molecules since the computational effort increases as n^3 with the number of electrons, n, as opposed to n^4 for the HF method or n^5 for configuration–interaction techniques. The scope of density functional based methods has further been enhanced to include pseudopotentials,[52] relativistic effects,[53] as well as energy gradients of use in geometry optimization.[45e,54] The existing program packages[47,48] are still not as user friendly, or readily available,[7b] as their ab initio counterparts and much development work remains to be done. Information about the various implementations is given in Scheme III.

SCHEME III

Methodology based on Approximate DFT

MS-Xα 1966	MS-Xα : Makes use of partial waves as basis (37). Relatively fast. Good for ionization potentials and excitation energies (10). Total energies unreliable (39). No geometry optimization. Full use of symmetry. Has relativistic extension (53f). Makes use of muffin-tin approximation (38). Developed by K.H. Johnson (37) .
DVM 1970	DVM: Makes use of numerical atomic orbitals or STO's. Avoids muffin-tin approximation by fit of density (45a). Accurate total energies (76d). Relativistic extension (53e). Numerical integration of matrix elements by Diophantine integration (40). Developed by Ellis and Painter (40). Extensive improvements by Delley (DMol-program) including new integration scheme (46c) and geometry optimization.
HFS-LCAO 1973	HFS-LCAO: Makes use of STO's. Accurate potentials (41). Full use of symmetry. Relativistic extensions (53a,b). Highly vectorized (47). Accurate total energies (49). Geometry optimization (54c). Accurate numerical integration (46b). Many auxiliary property programs . Pseudopotentials (52e,d). Embedding procedures (76h). Energy decomposition scheme (72). Developed by Baerends, Snijders, Ravenek, Vernooijs and te Velde (41,53,47,46d)
LCMTO 1974	LCMTO: Makes use of muffin-tin orbitals as basis. Calculates total energies. Developed by Gunnarson, Harris and Jones (44).
LCGTO-LSD 1976	LCGTO-LSD: Makes use of GTO's. Fit of exchange-correlation and Coulomb potential (43). Analytical calculation of matrix elements (48b). Accurate energies. Geometry optimization (54b,h). Strongly vectorized (48b). First developed by Sambe (42) as well as Dunlap (43). Extensive improvements by Salahub (DMon-program) and Andzelm (48b) (DGauss-program) as well as Rösch (74e). Also work by Pederson (45e) and Painter (45d)
NUMOL 1982	NUMOL: Unique basis set free program (50a,e). Accurate numerical integration (46e). Efficient generation of Coulomb potential (50c). Geometry optimization. Developed by Becke (50).
PL-DFT 1988	PL-DFT: Makes use of plane waves and pseudo potentials. Scales as N with number of electrons. Greats potential. Developed by Teter (69f)

III. Assessment of Approximate Density Functional Theory

We have in the previous sections discussed approximate expressions for the exchange–correlation energy. The expressions can in general be justified by referring to global properties of the spherically averaged hole–correlation function. They are in addition given in terms of the electron density in the spirit of DFT. The explicit dependence of the exchange correlation energy on the electron density renders approximate DFT considerable computational expediency with a wide range of applications. It remains, however, to be seen how well theoretical values based on approximate DFT calculations compare with experimental data and results from ab initio methods. This section is concerned with the quality of numerical results obtained by approximate DFT. It will in particular be of interest to establish whether the approximate representation of E_{XC} is adequate for properties involving energy differences such as bond energies, molecular structures, ionization potentials and excitation energies. We shall in addition try to assess the different levels of approximate DFT and the kind of improvements one might obtain by resorting to more refined theories.

A. Bond Energy Calculations

We shall begin our assessment of DFT-based methods by considering the calculation of bond dissociation energies. Results from this type of calculation should provide a clear indication of how well approximate DFT can account for molecular energetics. Of particular interest are the results obtained from the field of organometallic chemistry where the dearth of reliable experimental data is felt strongly. Accurate theoretical data in this area could afford a much needed supplement to the sparse available experimental data on metal–ligand bond energies, necessary for a rational

TABLE III. Bond Dissociation Energies (eV) for Diatomic Molecules

	expt[a]	HF[b]	HFS[c]	LDA[d]	LDA - NL[e]	HF + LC[f]	HF - PD[g]	HF - PD + LC[h]
B_2	3.1	0.9	3.9	3.9	3.2	1.2	1.3	1.6
C_2	6.3	0.8	6.2	7.3	6.0	2.0	2.3	3.5
N_2	9.9	5.7	9.3	11.6	10.3	7.4	7.3	9.3
O_2	5.2	1.3	7.1	7.6	6.1	2.2	2.9	3.7
F_2	1.7	-1.4	3.2	3.4	2.2	-0.7	0.7	1.4

[a] Reference 50a. [b] Hartree–Fock calculations.[50a] [c] Hartree–Fock–Slater calculations[50b,43a,b] with $\alpha_{ex} = 0.7$. [d] LDA calculations[11c] with $\alpha_{ex} = 0.66$d. [e] LDA calculations[11c] plus nonlocal corrections to exchange[23d] and correlation.[25] [f] Calculations[34] based on HF as well as local correlation.[33a] [g] Calculations[34] based on a proper dissociation wave function. [h] Calculations[34] based on a proper dissociation wave function with local correlation correction.[33a]

TABLE IV. First Metal–Carbonyl Dissociation Energy[a] in a Number of Metal Carbonyls

molecule	HFS[b]	LSD[b]	LSD/NL[c]	expt[c]
$Cr(CO)_6$	278	276	147	162
$Mo(CO)_6$	226	226	119	126
$W(CO)_6$	247	249	142	166
$Ni(CO)_4$	194	192	106	104

[a] All energies are kJ/mol. [b] V. Tschinke, unpublished results. [c] Reference 58.

approach to the synthesis of new transition-metal complexes.

Table III compares bond energies calculated by various methods with experiment for a number of homonuclear diatomic molecules. The Hartree–Fock scheme (HF) is seen to underestimate the bond energies uniformly. The discrepancy is especially large for the sample of multiple-bonded molecules considered here. The disagreement is less pronounced for species with a single σ-bond.[29b,62] It is by now very well known why the HF scheme represents π-bonds so poorly.[55,29b,32] Basically,[29b] the molecular hole–correlation function $\bar{\rho}^{\gamma\gamma}_{xHF}(\vec{r}_1, s)$ differs considerably from its atomic counterpart for certain $\vec{r}_1$ where it is too diffuse as a function of the interelectronic distance s.

The bond energies calculated by the HFS method,[43,50b] in which E_{xc} is represented by E_X^{LDA} of eq 7 and α_{ex} taken to be 0.7, are on the other hand in reasonable accord with experiment. The success of the HFS scheme can be attributed[29b] to the fact that $\bar{\rho}^{\gamma\gamma}_{x\alpha}(\vec{r}_1, s)$ changes little in the transition from atoms to molecule. We note that the HFS scheme tends to overestimate bond energies slightly. It is important in bond energy calculations to carry out spin-polarized calculations on the atoms, as pointed out by Dunlap[43b] et al.

The HFS scheme lacks correlation between electrons of different spins. This type of correlation is introduced in the LDA energy expression of eq 6. It follows from Table III that the LDA method affords even larger bond energies than the HFS scheme. The LDA method adds correlation between electrons of different spins to the HFS energy expression. Correlation between electrons of different spins is roughly proportional to the number of spin-paired electrons. This type of correlation is as a consequence more important (stabilizing) in the molecule than in the constituting atoms since the molecule in most cases have more spin-paired electrons than the constituting atoms. The correlation term E_C^{LSD} will as a result increase the bond energy compared to the HFS method. The tendency of either HFS or LDA to overbind is underlined further in Table IV where we present theoretical values[58] for the first CO dissociation energy in a number of metal carbonyls. Both HFS and LDA are seen to overestimate the M–CO bond strengths by nearly 100%. A deviation of this magnitude is clearly unacceptable in reactivity studies. In fact, it seemed in the last part of the 70's and the early part of the 80's as if approximate density functional methods would be unable to deal with chemical energetics.

This situation was changed by the development of gradient-based corrections due to Becke,[23d] Perdew,[25] and others.[23] Thus, adding the nonlocal exchange[23d] and correlations[25] corrections to the LDA energy expressions improves considerably the agreement between theory and experiment (Tables III and IV). The largest effect comes from the nonlocal correction to the exchange, whereas the influence of the nonlocal corrections to the correlation term is rather modest. The influence of the nonlocal exchange correction, E_X^{NL} is important in the tail of the valence density where the local exchange hole incorrectly has its maximum around the reference electron rather than at larger values[19] of the interelectron distance s. This error is corrected in the nonlocal theory by E_X^{NL} which tends to lower the total energy. On bond formation, parts of the valence tail disappear as the two atoms are brought together. The term E_X^{NL} is as a consequence more important (stabilizing) in the constituting atoms than in the combined molecule. Thus, the overall influence of E_X^{NL} on the bond energy is to reduce it in magnitude (Tables III and IV). The nonlocal correction is also important in the regions between two core shells. Contributions to the bond energy from these regions are crucial if the bond formation involves promotion of electron density from s-type orbital sto p-type orbitals.[19,29c]

Also presented in Table III are bond energies based on calculations (HF+LC) in which E_C^{LDA} has been added to E_X^{HF} according to eq 13. As mentioned previously, the E_C^{LDA} term only includes dynamic correlation, it does not correct for the near-degeneracy errors introduced by HF. Thus, bond energies based on $E_X^{HF} + E_C^{LDA}$ suffer from the same deficiencies as bond energies evaluated by the HF method.

The near degeneracy error can be corrected by introducing a limited proper dissociation configuration interaction (PD). It follows from Table III that the results based on HF+PD+LC are of nearly the same quality as those obtained from the LDA calculations with nonlocal corrections (LDA-NL). The combination of limited CI with correlation corrections derived from approximate density functional expressions is attractive from both a theoretical and practical point of view. It allows one to treat a number of electronic systems in which more than one determinantal wave function is required even in a zero order. Examples of such systems include spin and space multiplets as well as transition states of symmetry forbidden reactions. This

TABLE V. A Comparison of Bond Distances (Å) from HF and HFS Calculations with Experiment

	A–B	HF	HFS	expt
$Fe(CO)_5$	$Fe–C_{ax}$	2.047[a]	1.774[d]	1.807
	$Fe–C_{eq}$	1.874[a]	1.798[d]	1.827
$Fe(C_5H_5)_2$	Fe–C	1.88[b]	1.60[e]	1.65
$HCo(CO)_4$	$Co–C_{eq}$	2.02[c]	1.753[f]	1.764
	$Co–C_{ax}$	1.96[c]	1.779[f]	1.818

[a] Reference 64a. [b] Reference 64b. [c] Reference 64c. [d] Reference 66a. [e] Reference 66b. [f] Reference 66c.

kind of systems is not well represented[57] by the HFS and LDA methods or their nonlocal extensions. It is further able to take the dynamic correlation into account in a economical and efficient way through E_C^{LDA} or similar expression.[33] An ab initio description[31] of dynamic correlation requires a substantial amount of configurations for small systems and is virtually out of reach for larger size molecules. The HF+PD+LC method has been pioneered by Clementi,[33a] Savin,[33c] and others.[33]

It seems at the present time that the LDA method augmented with nonlocal exchange and correlation corrections (LDA-NL) represents the most efficient and accurate method for the evaluation of bond energies within the density functional framework. Calculations on metal carbonyls,[58] binuclear metal complexes,[59] alkyl and hydride complexes,[60] as well as complexes containing M–L bonds for a number of different ligands,[61] have shown that LDA-NL afford metal–ligand and metal–metal bond energies of nearly chemical accuracy (±5 Kcal mol^{-1}). Becke[50d,e] has recently carried out accurate basis set free calculations on the bond energy in a number of smaller molecules. Calculations in which relativistic effects are taken into account[52a] have also appeared.[60c–d]

B. Molecular Structures

It has in recent years been possible to determine molecular structures by theoretical methods with increasing accuracy. Of particular importance in this development has been the implementation[62,63c] of automated[63b] procedures based on analytical expressions[63d–e] for the energy gradient. It is now routine[62] to carry out geometry optimizations of organic molecules based on HF or correlated ab initio methods with an accuracy of ±0.02 Å, or better, for bond distances. The application of ab initio methods, in particular on the HF level, has been less successful in the area of transition-metal chemistry.[64] This is illustrated by Table V where metal–carbon distances calculated by the HF method[64] with large basis sets are displayed for three representative organometallic molecules. The metal–carbon bond distances calculated by the HF method are seen to be too long by up to 0.2 Å. The method gives in addition, in the case of $Fe(CO)_5$, a large difference of 0.2 Å between axial and equatorial bonds, which is not observed experimentally. The inability of the HF method to supply reliable structural data for transition-metal complexes can, as in the case of bond energies, be traced back to the near degeneracy error as discussed by Lüthi et al.[64a] The deficiency of the HF method can be removed by configuration interaction methods.[64] However, such methods are costly and less amenable to automated geometry optimization procedures based on analytical expressions.

TABLE VI. Bond Lengths (Å) for Some Diatomic Molecules

	expt[a]	HF[b]	HFS[c]	LDA[d]	LDA-NL/ X[e]	LDA-NL/ XC[f]
B_2	1.59		1.60	1.60	1.62	1.62
C_2	1.24	1.25	1.24	1.24	1.25	1.25
N_2	1.10	1.06	1.09	1.09	1.10	1.10
O_2	1.21	1.15	1.20	1.20	1.23	1.22
F_2	1.41	1.32	1.38	1.38	1.44	1.41

[a] Reference 50a. [b] Reference 43. [c] Calculations from ref 50a based on eq 11a with $\alpha_{ex} = 0.7$. [d] Calculations from ref 11c based on eq 13 with $\alpha_{ex} = 2/3$. [e] Calculations from ref 11c based on LDA with nonlocal exchange corrections.[23d] [f] Calculations from ref 11c based on LDA with nonlocal exchange[23d] and correlation[25] corrections.

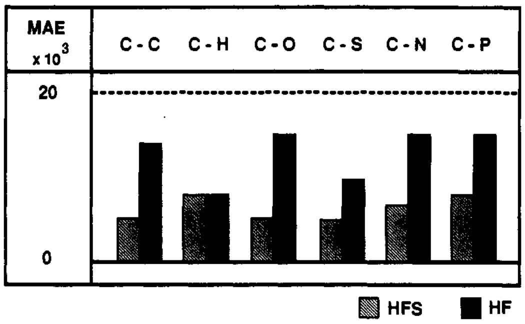

Figure 3. Mean absolute errors from HFS and HF calculations on bond distances (Å).

Early HFS calculations[49,43,65,50] on bond distances in diatomic molecules gave quite encouraging results (Table VI). They indicated that methods based on approximate DFT might be quite accurate for geometry optimizations. Thus, both HFS and LDA are seen to give bond distances in better accord with experiment than HF (Table VI). The HFS and LDA schemes afford in most cases quite similar results. However, there are examples, such as Li_2 and Na_2, in which LDA is in much better agreement with experiment than HFS. The simple HFS method is further seen to afford reasonable estimates[66] for the metal–carbon distances in Table V. The HFS method appears to underestimate metal–ligand bond distances by up to 0.05 Å. This situation is apparently not improved significantly by resorting to LDA calculations.[69c] The inclusion of nonlocal correction to the exchange term[23d] (LDA-NL/X) tends to elongate the bond,[11c] whereas the nonlocal correction to correlation[25] seems[11c] to shorten the bonds. Much work is still required in order to evaluate the influence of nonlocal corrections on geometrical parameters.

Approximate density functional methods have, however, in spite of the encouraging results of Tables V and VI not been used to the same degree as the HF method in geometry optimizations. This is primarily because geometry optimizations by the HFS method until recently were carried out with a laborious point by point tracing of the potential surface as a function of the nuclear coordinates. The HF programs have on the other hand utilized automated procedures based on analytical expressions for the energy gradients for a long time.

This situation has now changed with the derivations of analytical expressions for the energy gradients within the density functional formalism[54] and their implementation[54b,c,h,69e] and integration into general purpose programs.[47c,48c–f,50f] Numerous calculations on molecular structures have appeared over the past few years.[67,68a,66d] Figure 3 summarizes the experience[54c,66d] gained from calculations on organic molecules. It follows from Figure 3 that the bond distances from HFS calculations are in at least as good agreement with experiment as the bond distances calculated by the HF method. The errors range, in the HFS case, from 0.01 Å for C–N and C–P bonds to 0.005 Å in C–C and C–O bonds. The HFS method seems in particular to fare well for double and triple bonds. The error range for bond angles calculated by the HFS method is 1–2°. Very recent calculations by Andzelm[69a] and Pederson[69b] indicate that geometrical parameters optimized by LDA are of the same quality as parameters optimized by the MP2 ab initio method[63e] for organic molecules. Dixon[69c] has carried out a comprehensive study of fluorinated alkanes and silanes. Calculations[54c] on some 30 inorganic molecules of main group elements revealed a deviation of 0.01 Å for bond distances and 1° for bond angles. The errors in calculated HFS and LDA metal–metal and metal–ligand bond distances of transition-metal complexes are as large as 0.05 Å. However, this error is still smaller than the deviations encountered in HF calculations. It remains to be seen whether more advanced theories, in which nonlocal corrections are taken into account, will be able to supply more accurate geometrical parameters for transition-metal complexes.

C. Potential Energy Surfaces and Conformational Analysis

There have been a number of HFS or LDA studies on the relative stability of isomers and conformers. These include the relative energies of eclipsed and staggered conformations in $Fe(C_5H_5)_2$,[69c] C_2H_6,[69c] as well as a number of binuclear metal complexes.[70a] Conformational energy differences seem[69c] to be well represented by HFS or LDA. The energetics for different coordination modes of ligands complexed to transition metals have been studied for phosphaalkene,[71a] F_2 and H_2,[71b] alkenes and alkynes,[71c,d] BH_4^-,[71e] O_2,[71d] X_2, CX_2 (X = O, S, Se, Te),[71f,g] carbocycles,[71i] as well as H.[71h] A special energy decomposition scheme has been devised[72,49,71c] which breaks down the coordination energy of a ligand into steric and electronic factors. This scheme makes it possible to explain interaction energies as well as conformational preference of a ligand in terms of well-established chemical concepts. As examples, the decomposition analysis is able to provide estimates of the respective contributions from the σ, π, and δ components in binuclear complexes[59,70] with multiple bonds: **1a**, the relative importance of donation and backdonation in transition-metal complexes of unsaturated ligands[71] such as olefins; **1b**, the contributions[71h] to the protonation energy; **1c**, from the pure electrostatic interaction of the proton as well as the charge rearrangement following the formation of the protonated complex.

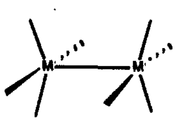

1a

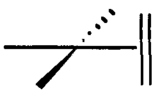

1b

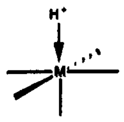

1c

The HF method represents conformational energies of saturated systems, such as rotation barriers in alkanes, quite well. It is not likely that HFS or LDA will afford substantially different results for this type of systems. However, examples are known among unsaturated systems in which HF- and LDT-based methods differ. Thus, HF[64c] finds $HCo(CO)_4$ of C_{2v} symmetry, with hydrogen in an equatorial position, to be more stable than the experimental observed C_{3v} structure where hydrogen is in the axial position. On the other hand, HFS[66c] finds the C_{3v} structure to be the more stable conformation.

Salahub,[48b,73,69d] Rösch,[66a,74] Dunlap,[74,75] Delley,[68b] and Baerends[76] have studied the structure of metal clusters and their interaction with atoms and small molecules. These investigations include studies on the geometrical and electronic structure of small naked metal clusters[48b,78a,80d] as well as their interaction with CO,[77,79c,80a–d,73c,75a] O_2,[80g,73b] hydrogen,[69a,d,48b,73d] and alkaline atoms.[78a] Of particular interest has been the metal–metal bond strength and electronic structure of M_2 (M = Cr, Mo, W)[68a,73e,59] where DFT-based methods have proven more accurate then standard ab initio techniques. Cluster calculations have also been applied to simulate scattering from surfaces[77] as well as interfaces.[78,68d] Studies have further been carried out on polymers[79] such as *trans*-polyacetylene[79a–c,66c] and polysilane.[83b] Ravenek[76h] has developed an embedding method for calculation in which small clusters are used to simulate surfaces or larger aggregates.

D. Transition-State Structures and Reaction Profiles

The complete characterization of a chemical reaction requires the full determination of the potential energy surface for the reaction system as a function of the nuclear coordinates. In the classical transition-state theory this requirement is reduced to a determination of the surface around the reactant(s), the product(s), the transition state (saddle point), and the lowest energy pathway connecting them.

The first determination of a transition-state structure based on approximate DFT has appeared recently. Fan and Ziegler[80] studied the isomerization reaction $CH_3NC \rightarrow CH_3CN$. The energy barrier for the process has been determined experimentally[81] with high accuracy as 38.4 kcal mol^{-1}. The barrier calculated by the HFS method is 40.8 kcal mol^{-1}. The best ab initio calculation[82] based on SDQ-MBPT(4) with 10^7 configurations gave a barrier of 41 kcal mol^{-1}. More calculations are clearly needed to provide a full assessment of how well approximate DFT methods represent transition-state structures and activation barriers. Such calculations should not only involve other types of reactions but also more accurate approximate DFT methods than the simple HFS scheme.

A number of reaction profiles[66c,d,83] for key steps in processes catalyzed by transition-metal complexes have been traced approximately by a linear transit procedure. A complete analysis[66c,68,73d–g] has been provided for all the steps in the hydroformylation process catalyzed by $HCo(CO)_4$. This analysis presents in addition a critical evaluation[66c,66] of HF studies carried out on the same process. It is concluded[66c,68] that the HF method, which in transition-metal systems represents bond energies

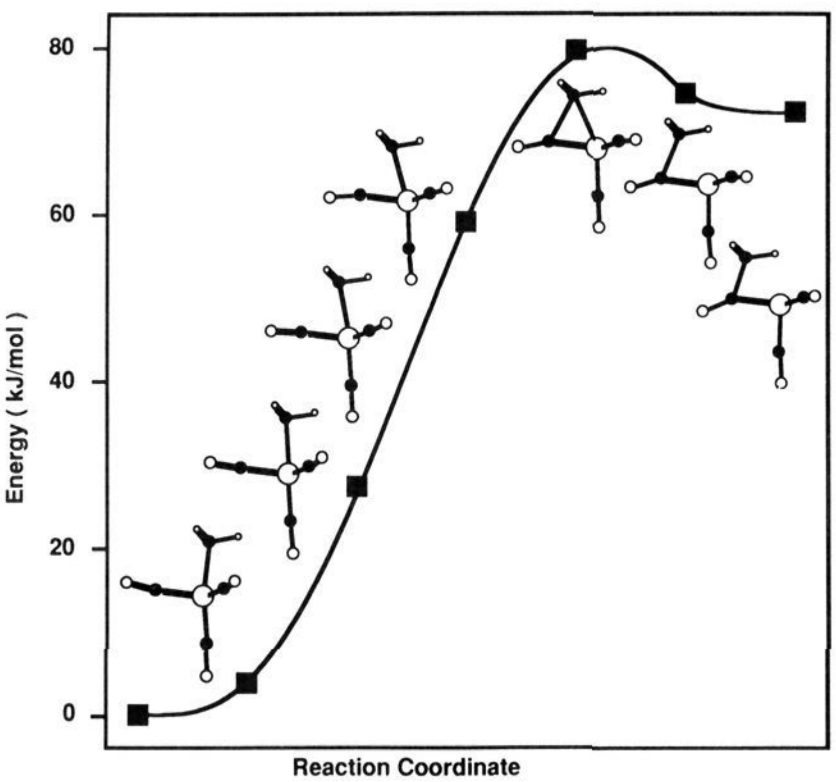

Figure 4. Reaction profile for the migration of a methyl group in $CH_3Co(CO)_4$ to a cis CO ligand to form $CH_3(O)CCo(CO)_3$.

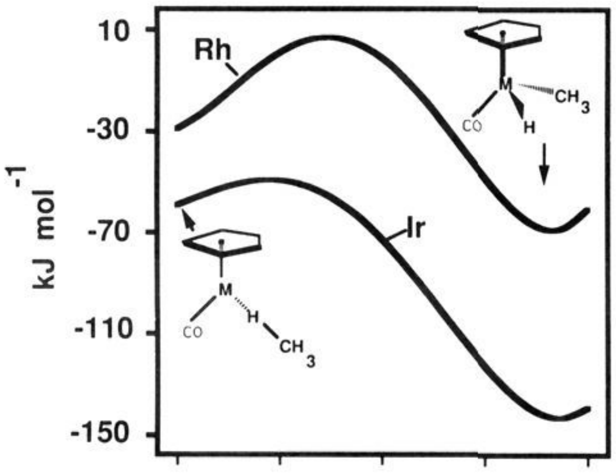

Figure 5. Reaction profile for the oxidative addition of CH_4 to the rhodium center in Cp(CO)Rh.

and geometries poorly, is inadequate for reactivity studies involving transition-metal complexes. Figure 4 displays as an example the reaction profile[66c] for the methyl migration reaction **2a** → **2b** which is a key step in the hydroformylation process. The profile in Figure 4 seems to agree with available experimental[83h] data. Also given in **2a** and **2b** are the optimized structures of the two species created when the HFS method is used.[66c]

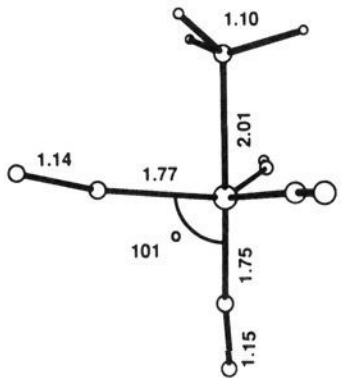

2a

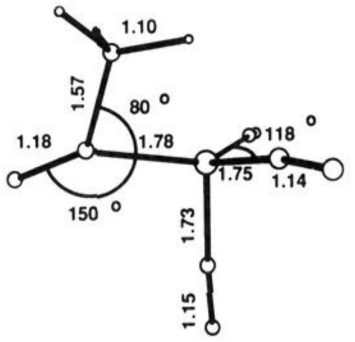

2b

Another example involves the activation of the C–H bond in methane[83i] by the coordinatively unsaturated CpIr(CO) and CpRh(CO) complexes (Figure 5). This reaction, **3a** → **3b**, could serve as an important step in the functionalization of methane to more valuable chemicals. The reaction profiles of Figure 5 reproduce many of the observed trends[83i] including a low activation barrier and a tendency for iridium to activate the C–H bond more readily than rhodium. The first stage of the reaction is represented by the formation of a weak methane adduct, **3a**, followed by the formation of a transition state, **3c**, with an elongated C–H bond, and finally the hydrido alkyl product, **3b**. Also shown in **3a**, **3b**, and **3c** are the optimized structures of the three species using the HFS method.[83i]

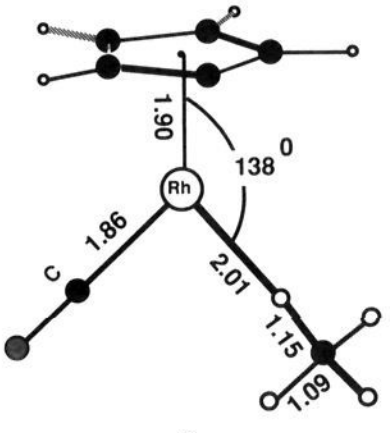

3a

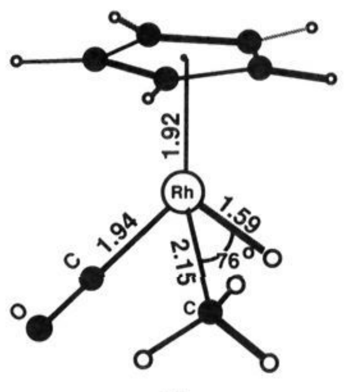

3b

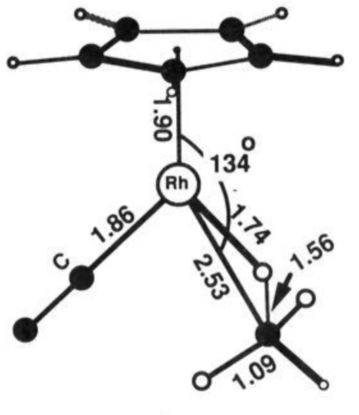

3c

E. Molecular Force Fields

The construction of molecular harmonic force fields from experimental data (based on infrared and Raman spectroscopy) have benefited considerably over the past decade from new developments in computational chemistry. Thus, Pulay[84] has with his force method, in which force fields and vibrational frequencies are evaluated from a numerical differentiation of analytical energy gradient calculated by ab initio methods, been able to study a number of small molecules. The studies by Pulay have more recently been augmented by investigations in which the second derivatives[63e] of the total energy with respect to nuclear displacements were calculated analytically.

Calculations of frequencies and force fields on the Hartree–Fock level of theory are now carried out almost routinely[62] although the basis sets employed in calculations on large-size molecules often are somewhat restricted as the computational effort in HF calculations increases as M^4 with the number of basis functions M. Frequency and force field calculations in which correlated ab initio methods have been employed are still restricted to small-size molecules and the evaluation of first and, in particular, second derivatives of the energy by such methods are rather demanding.

Table VII displays vibrational frequencies for a number of diatomic molecules. It is clear that HF differ significantly from experiment in particular for the π-bonded systems C_2, CO, and N_2. The failure of HF in

TABLE VII. Harmonic Frequencies (cm^{-1}) for Diatomics

	HF	HFS	LDA	LDA/NL	MP2	expt[g]
C_2	1970[a]	1870[d]	1880[h]	1830[i]		1855
N_2	2730[a]	2380[d]	2380[h]	2330[i]	2173[f]	2358
CO	2430[a]	2170[d]			2113[f]	2170
AuH	1875[b]	2305[e]				2241
Au_2	165[c]	201[e]				191

[a] Yoshimine, M.; McLean, A. D. *Int. J. Quantum Chem.* **1967**, *S1*, 313. [b] Lee, Y. E.; Ermler, W. C.; Pitzer, K. S.; McLean, A. D. *J. Chem. Phys.* **1979**, *70*, 293. [c] Hay, P. J., Wadt, W. R.; Kahn, L. R.; Bobrowicz, F. W. *J. Chem. Phys.* **1978**, *70*, 293. [d] Reference 50a. [e] Reference 60d. [f] Reference 62. [g] Huber, K. P.; Herzberg, G.; *Molecular Spectra and Molecular Structure*; Van Nostrand Reinhold; New York, 1979. [a] Reference 11c. [i] LDA with nonlocal corrections to exchange[23d] and correlation.[25]

TABLE VIII. Frequencies Obtained by HFS, HF, and Experiment[a]

mol	symmetry	HFS	HF[b]	MP2[b]	expt
H_2O	a_1	3814 (−18)[c]	4070 (238)[c]	3772 (−60)	3832[d]
	a_1	1590 (−58)	1826 (178)	1737 (89)	1648
	b_1	3877 (−66)	4188 (245)	3916 (−27)	3943
H_2S	a_1	2631 (−91)	2918 (196)	2797 (75)	2722[e]
	a_1	1178 (−37)	1368 (153)	1279 (64)	1215
	b_1	2644 (−89)	2930 (197)	2824 (91)	2733
NH_3	a_1	3314 (−192)	3690 (184)	3504 (−2)	3506[f]
	a_1	953 (−69)	1207 (185)	1166 (64)	1022
	e	3468 (−109)	3823 (246)	3659 (82)	3577
	e	1564 (−127)	1849 (158)	1852 (161)	1691
PH_3	a_1	2313 (−139)	2666 (214)	2510 (58)	2452[f]
	a_1	950 (−91)	1143 (102)	1079 (38)	1041
	e	2329 (−128)	2602 (145)	2526 (69)	2457
	e	1088 (−66)	1278 (124)	1181 (27)	1154
CH_4	a_1	2951 (−186)	3197 (60)	3115 (−22)	3137[f]
	e	1467 (−100)	1703 (136)	1649 (38)	1567
	t_2	3102 (−56)	3302 (144)	3257 (99)	3158
	t_2	1236 (−121)	1488 (131)	1418 (61)	1357
SiH_4	a_1	2187 (−190)	2233 (−144)	2323 (−14)	2377[g]
	e	905 (−70)	1052 (77)	1005 (30)	975
	t_2	2217 (−102)	2385 (66)	2337 (18)	2319
	t_2	777 (−168)	1016 (71)	956 (11)	945
C_2H_4	a_g	3063 (−90)	3344 (191)	3231 (78)	3153[h]
	a_g	1647 (−8)	1856 (201)	1724 (69)	1655
	a_g	1348 (−22)	1499 (129)	1424 (54)	1370
	a_u	972 (−72)	1155 (111)	1083 (39)	1044
	b_{1g}	3138 (−94)	3394 (162)	3297 (65)	3232
	b_{1g}	1209 (−36)	1353 (108)	1265 (20)	1245
	b_{1u}	908 (−61)	1095 (126)	980 (11)	969
	b_{2g}	879 (−80)	1099 (140)	931 (−28)	959
	b_{2u}	3170 (−64)	3420 (186)	3323 (89)	3234
	b_{2u}	814 (−29)	897 (54)	873 (30)	843
	b_{3u}	3041 (−106)	3321 (174)	3222 (75)	3147
	b_{3u}	1399 (−74)	1610 (137)	1523 (50)	1473

[a] The unit is cm^{-1}. [b] HF/6-31G* calculations. See ref 62. [c] Deviations from harmonic experimental values are given in the parentheses. [d] Strey, G. *J. Mol. Spectrosc.* **1967**, 24, 87. [e] Allen, H. C., Jr.; Plyler, E. K. *J. Chem. Phys.* **1956**, *25*, 1132. [f] Duncan, J. L.; Mills, L. M. *Spectrosc. Acta* **1964**, *20*, 523. [g] Levin, I. W.; King, W. T. *J. Chem. Phys.* **1962**, 37, 1375. [h] Duncan, J. L.; McKean, D. C.; Mallison, P. D. *J. Mol. Spectrosc.* **1973**, *45*, 221.

C_2, CO, and N_2 illustrates once again the inadequacy of HF in multibonded systems due to the inherent near-degeneracy error.[55,29b] This error is to a large degree eliminated by MP2,[62] in which electron correlation is taken approximately into account. The MP2 method brings the calculated frequencies in much closer agreement with experiment (Table VII). The HFS scheme is seen on the whole to give a good representation of the frequencies, even for the two transition-metal systems AuH and Au_2. The introduction of dynamic correlation (LDA) does not significantly change the theoretical results. Few data are available on the way in which nonlocal (LDA/NL) corrections to exchange[23d] and correlation[25] influence frequencies. The few available data[11c] points to a rather modest influence (Table VII).

DFT-based methods have in spite of the encouraging results presented in Table VII not been used to nearly the same degree in frequency calculations as the HF scheme. This is primarily so because frequencies obtained from DFT calculations were calculated from a laborious point by point tracing of the potential energy surface as a function of the nuclear coordinates, whereas ab initio programs,[62] as already mentioned, utilize powerful automated procedures based on analytical expressions for the first[84] (and second[63e]) energy derivatives.

The recent implementations of energy derivatives[54b,c] within the DFT frame work makes it now tractable[80,85] to evaluate frequencies from a numerical differentiation of the energy gradients in the spirit of Pulay's force method.[84] Harmonic frequencies calculated by the HF, MP2, and HFS methods for H_2O, H_2S, NH_3, PH_3, CH_4, SiH_4, and C_2H_4 are in Table VIII compared to experimental data, with deviation between calculated and experimental values given in parentheses. It is evident from Table VIII that the harmonic frequencies obtained by the HFS method[85a] are somewhat too small compared to experiment, whereas the HF method afford too high values. The average percentage deviation of the harmonic frequencies calculated by the HFS method varies from 1.9% in the case of H_2O to 9.3% for SiH_4. The corresponding deviation of the HF results are for all molecules except SiH_4 higher. The mean absolute deviation of all frequencies listed in Table VIII is 5.0% in the HFS case as opposed to 9% in the HF case. The LDA method afford,[85b] for the same sample of points, frequencies quite close to those obtained by HFS.[85a] The frequencies calculated by the MP2 method has a mean absolute deviation of 4% and are thus slightly better than the DFT results. Salahub[85b] et al. have calculated frequencies for the same sample of molecules given in Table VIII. Their results are surprisingly similar to the HFS frequencies (±30 cm^{-1}).

The data in Tables VII and VIII would indicate that DFT-based methods on the whole are able to furnish relatively accurate harmonic frequencies. They should thus over the next decade be able to supply valuable information about molecular force fields, in particular for transition-metal complexes and metal clusters. In fact, Salahub[85a] et al. have quite recently obtained frequencies for organic molecules interacting with metal clusters. This type of calculations can provide crucial information in connection with studies of chemisorption.

The use of DFT in studies on molecular force fields would be greatly enhanced by the employment of analytical second derivatives. Expressions[86] for the second and third derivatives can be derive in a manner[63e] quite similar to that employed for HF theory. However, a practical implementation of second derivatives within DFT has not yet been achieved.

F. Ionization Potentials

Photoelectron spectroscopy (PES) emerged in the early 70's as a new and exciting technique with direct bearings on molecular orbital energies. It is thus not surprising that PES has served as a testing ground for

TABLE IX. Ionization Energies (eV)

	HFS[b]	LDA[b]	LDA/NL[b]	expt[a]
N_2	14.60	15.05	15.24	15.60
	16.6	16.95	16.81	16.98
CO	12.81	13.50	13.85	14.01
	16.71	17.17	17.01	16.53
F_2	14.78	15.02	15.34	15.70
	18.08	18.35	18.58	18.98
H_2O	12.03	12.55	12.59	12.62
	13.95	14.46	14.60	14.75
NH_3	10.06	10.62	10.76	10.88
	15.59	15.98	16.37	16.0
CH_4	13.18	13.61	14.01	14.35
	21.20	21.50	22.00	23.00
C_2H_4	10.14	10.60	10.56	10.51
	11.84	12.22	12.75	12.85

[a] Turner, D. W. *Molecular Photoelectron Spectroscopy*; Wiley: New York, 1980. [b] Reference 29d.

new and increasingly sophisticated theoretical methods including DFT-based schemes. In fact, one of the first successful applications of the HFS method in chemistry involved the assignment of photoelectron spectra. The early work based on the SW-Xα method has been reviewed by Connolly[10a] and Case,[10b] whereas Baerends[87] has reviewed work on HFS calculations without the muffin-tin approximation.

Table IX displays the first and second ionization potential for a number of smaller molecules. The HFS method underestimates[29a,c–d] in general ionization potentials for systems where the molecule has a closed-shell structure and the ion has a single unpaired electron. Introduction of dynamic correlation by resorting to LDA is seen (Table IX) to increase the calculated ionization potentials and thus close the gap between theory and experiment. The increase in the calculated ionization energy due to E_C^{LSD} can readily be understood when we recall that correlation will stabilize the molecule relative to the ion since the former has one additional pair of electrons with opposite spins. A number of HFS calculations on ionization potentials have been carried out in the closed-shell formalism (R-HFS), although the ion has one open shell. R-HFS affords a better agreement with experiment than unrestricted calculations (U-HFS) since the ion is of higher energy in R-HFS compared to U-HFS. However from a theoretical point of view, one should always apply the unrestricted formalism to open-shell systems in DFT methods.

The nonlocal corrections to exchange are seen to bring about a small but significant improvement of the theoretical ionization potentials (Table IX). The influence of Becke's exchange correction has been studied elsewhere.[29a,c–d] It is, in particular, important for ionizations out of orbitals with a substantial contribution from atomic s-type orbitals.

There have been several recent applications of approximate DFT to photoelectron spectroscopy[48b,87] including some in which relativistic effects[88] have been taken into account. An extensive investigation[70c,d] combining the calculation of bond distances and PE-spectra involves the binuclear complexes $M_2(O_2CR)_4$ and $M_2Cl_4(PR_3)_4$ ($M = Cr, Mo, W$) with a quadruple metal–metal bond. Their PE spectra (see Figure 6) reveal three bonds (A, B, and C) corresponding to an ionization out of the δ, π, and σ metal–metal bonding orbitals with the B band being considerably more broad than either A or C. The assignment of A, B, and C has been controversial.[70c,d] Approximate DFT calculations[70c,d] assign A, B, and C to δ, π, and σ, respectively. The potential energy surfaces in Figure 6 were, in addition, able to explain the broad feature of B in terms of a large change in the R_{MM} equilibrium distance for the π-ion state.

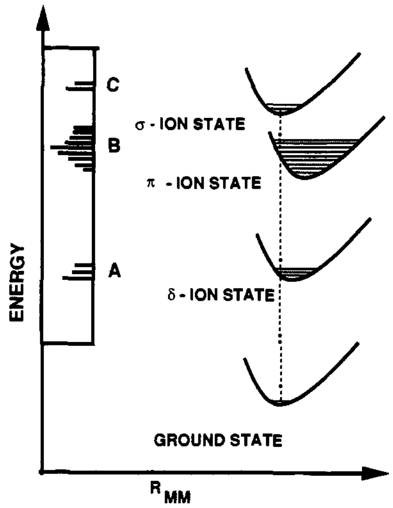

Figure 6. Schematic representation for the energy of the quadruple-bonded binuclear complex M_2L_{2n} in its ground state and first three ion states, corresponding to ionization out of the s, p, and d bonding orbitals, as a function of the metal–metal bond distance R_{MM} and schematic representation of the three first PE bands A, B, and C with their vibrational shapes.

Noodleman and Baerends[89] have revealed some unphysical features of DFT-based methods in connection with calculations on ionizations involving noninteracting symmetry-equivalent localized orbitals. As an example consider symtriazine (4) with three symmetry-equivalent nitrogen lone pairs, l_{a-c}. The ionization can be considered as localized with the electron hole confined entirely to one of the lone pairs, say l_a. Alternatively, one might consider the ionization to be delocalized with the electron hole spread over symmetrized combinations of l_{a-c}, transforming as a_1' or e′ in the D_{3h} point group. The localized hole state of the ion has usually a lower energy than the delocalized hole state in ab initio theory, as one might expect from physical arguments. DFT-based methods finds by contrast that the delocalized hole state is of lower energy than its localized counterpart. This unphysical result can be traced to an inadequate description of $\rho_{X\alpha}^{\gamma\gamma}(\vec{r}_1, s)$ in the delocalized case which leads to spurious self-interaction terms for the electrons. Noodleman and Baerends[89] have shown that one should apply the localized description in connection with approximate DFT calculations on ionizations out of localized and noninteracting symmetry-equivalent orbitals representing lone pairs or core shells.

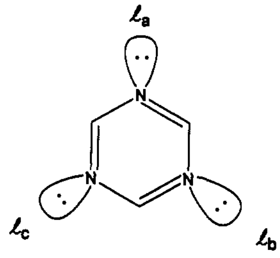

4

G. Multiplets, Excitation Energies, and Near Degeneracies

We have previously seen how most approximate DFT-based methods incorporate the exchange energy expression for the homogeneous electron gas into E_{XC} and the total energy. The particular form for $E_{\mathrm{X}}^{\mathrm{LDA}}$ has

$$E_{\mathrm{X}}^{\mathrm{LDA}} = -9/4\alpha_{\mathrm{ex}}[3/4\pi]^{1/3}\int\{[\rho_1^{\alpha}(\vec{\mathbf{r}}_1)]^{4/3} + [\rho_1^{\beta}(\vec{\mathbf{r}}_1)]^{4/3}\}\,\mathrm{d}\vec{\mathbf{r}}_1 \quad (22)$$

a number of features which makes it difficult to evaluate space and spin multiplets in an unambiguous way within approximate density functional theory. The problem can be illustrated[90] by considering the electron configuration $(a)^1(b)^1$ from which we can construct four determinantal wave functions

$$\mathrm{D}_1 = |\overset{+}{a}\overset{+}{b}| \qquad \mathrm{D}_2 = |\overset{-}{a}\overset{-}{b}| \qquad \mathrm{D}_3 = |\overset{+}{a}\overset{-}{b}| \qquad \mathrm{D}_4 = |\overset{-}{a}\overset{+}{b}|$$

The configuration gives rise to one triplet and one singlet with the spin eigenfunctions represented by

$$ {}_{1}^{3}\Psi = \mathrm{D}_1 \qquad {}_{0}^{3}\Psi = \sqrt{1/2}\{\mathrm{D}_3 + \mathrm{D}_4\}$$
$$ {}_{-1}^{3}\Psi = \mathrm{D}_2 \, {}_{0}^{1}\Psi = \sqrt{1/2}\{\mathrm{D}_3 - \mathrm{D}_4\}$$

A substitution of $\rho_1^{\alpha}(\vec{\mathbf{r}}_1)$ and $\rho_1^{\beta}(\vec{\mathbf{r}}_1)$ for the four spin states into $E_{\mathrm{X}}^{\mathrm{LDA}}$ affords the rather unphysical result $E_{\mathrm{X}}^{\mathrm{LDA}}({}_{1}^{3}\Psi) = E_{\mathrm{X}}^{\mathrm{LDA}}({}_{-1}^{3}\Psi) \neq E_{\mathrm{X}}^{\mathrm{LDA}}({}_{0}^{3}\Psi) = E_{\mathrm{X}}^{\mathrm{LDA}}({}_{0}^{1}\Psi)$. Thus one of the triplet components, ${}_{-1}^{3}\Psi$, is seen to have an exchange energy that differs from the two other component and is equal to the singlet ${}_{0}^{1}\Psi$. Ziegler[57b] et al. have shown that this apparent paradox can be resolved by realizing that $E_{\mathrm{X}}^{\mathrm{LDA}}$ only is applicable[57b] to a single determinantal wave function. Thus exchange energies for multiplets represented by linear combinations of determinants must be evaluated indirectly by Slater's sum rules. For the case at hand D_1 and D_2 afford directly the exchange energy for the triplets

$$E_{\mathrm{X}}^{\mathrm{LDA}}(\text{triplet}) = E_{\mathrm{X}}^{\mathrm{LDA}}(\mathrm{D}_1) = E_{\mathrm{X}}^{\mathrm{LDA}}(\mathrm{D}_2) \quad (23a)$$

The determinants D_3 and D_4 are equal mixtures of a triplet and a singlet. It follows thus from Slater's sum rules that

$$E_{\mathrm{X}}^{\mathrm{LDA}}(\mathrm{D}_3) = 1/2E_{\mathrm{X}}^{\mathrm{LDA}}(\text{triplet}) + 1/2E_{\mathrm{X}}^{\mathrm{LDA}}(\text{singlet}) \quad (23b)$$

which allows us to determine the singlet exchange energy as

$$E_{\mathrm{X}}^{\mathrm{LDA}}(\text{singlet}) = 2E_{\mathrm{X}}^{\mathrm{LDA}}(\mathrm{D}_3) - E_{\mathrm{X}}^{\mathrm{LDA}}(\mathrm{D}_1) \quad (23c)$$

Consider next the general case of a configuration which gives rise to a number of space and spin multiplets. Let the exchange energy of all different determinants, D_i, corresponding to the configuration be given as $E_{\mathrm{X}}^{\mathrm{LDA}}(\mathrm{D}_i)$ and let the exchange energies of the corresponding multiplets, M_i, be given by $E_{\mathrm{X}}^{\mathrm{LDA}}(\mathrm{M}_i)$. The two sets of energies are related by

$$E_{\mathrm{X}}^{\mathrm{LDA}}(\mathrm{D}_i) = \sum_j C_{ij}E_{\mathrm{X}}^{\mathrm{LDA}}(\mathrm{M}_j) \quad (24)$$

where the coefficients C_{ij} in most cases are given by group theory. The procedure for calculating multiplet energies by Slater's sum rules is now to invert the set of equations in eq 24 to

$$E_{\mathrm{X}}^{\mathrm{LDA}}(\mathrm{M}_j) = \sum_i A_{ji}E_{\mathrm{X}}^{\mathrm{LDA}}(\mathrm{D}_i) \quad (25)$$

TABLE X. Calculated Triplet (E_{T}) and Singlet (E_{S}) Transition Energies (eV)

compd	transition	E_{t}	$E_{\mathrm{t}}^{\mathrm{exp}}$	E_{s}	$E_{\mathrm{s}}^{\mathrm{exp}}$
H_2CO	$2b_2 \rightarrow 2b_1$	3.18[a]	3.21[a]	3.70[a]	3.50[a]
C_2H_2	$\pi \rightarrow \pi^*$	4.57	4.60	7.45	7.6
C_4H_6	$1b_g \rightarrow 2a_u$	3.31	3.22	5.05	5.9
CO	$5\sigma \rightarrow 2\pi$	5.81	6.3	7.99	8.4
N_2	$3\sigma_g \rightarrow 1\pi_g$	7.83	8.1	9.13	9.3
N_2	$2\sigma_g \rightarrow 1\pi_g$	10.68	11.1	12.34	12.8

[a] For reference to experimental and theoretical values see ref 57b. All calculations are based on the HFS method.

TABLE XI. Singlet Excitation[a] Energies for Tetrahedral d^0 Oxo Complexes in Electronvolts

	MnO_4^-		CrO_4^{2-}		VO_4^{3-}	
transition	E_{s}	$E_{\mathrm{s}}^{\mathrm{exp}}$	E_{s}	$E_{\mathrm{s}}^{\mathrm{exp}}$	E_{s}	$E_{\mathrm{s}}^{\mathrm{exp}}$
$t_1 \rightarrow 2e$	2.48	2.27	3.30	3.32	4.51	4.58
$4t_2 \rightarrow 2e$	3.96	3.47	4.58	4.53	5.71	5.58
$t_1 \rightarrow 5t_2$	4.15	3.99	4.90	4.86	6.15	6.15

[a] Reference 108b.

A detailed discussion of the conditions under which eq 24 can be inverted into eq 25 has been given elsewhere.[57b] Triplet and singlet excitation energies evaluated according to the procedure outlined above are given in Table X for a number of small molecules. The agreement with experiment is in general quite good. Slater's sum rules have also been applied by Von Barth[91] and Gunnarsson[92] to evaluate atomic multiplets. Alternative procedures for calculation of multiplet splittings within approximate DFT have been developed by Dunlap.[93]

The HFS scheme has been used extensively to calculate excitation energies and many of the applications have been reviewed.[10] An indication of the high accuracy usually obtained by approximate DFT methods is given in Table XI. This table presents HFS calculation on the three first excitations in the tetrahedral d^0 oxo complexes MnO_4^-, CrO_4^{2-}, and VO_4^{3-}. In particular the electronic spectrum of MnO_4^- has served as an acid test for new theoretical methods. It should be mentioned that HF and post-HF methods so far have failed to calculate the excitation energies of MnO_4^- with near quantitative accuracy. Buijse[55] and Baerends have recently analyzed the error sources in HF calculations on MnO_4^-.

There are cases other than multiplets in which the description of an electronic system requires more than one determinant, even at the lowest level of approximation. Examples include weakly interacting subunits, as encountered in dissociating bonds or magnetic-coupled metal centers, as well as avoided crossings of potential energy surfaces for states of the same symmetry in which the highest occupied and lowest unoccupied orbitals are of nearly the same energy. Dunlap[93,94] has developed a method in which avoided crossings of potential energy surfaces can be taken into account. The method has been applied to C_2, Si_2, Ni_2, as well as several small cluster systems. The method can also be applied to bond dissociations as illustrated[94b] by a calculation on H_2. Noodleman[95] et al. have developed a method to describe the magnetic coupling between weakly interacting metal centers. This method, which is based on spin-projection techniques, has been applied to several metal dimers[95a] as well as ferredoxin.[95c,d] It can potentially also be applied to bond dissociations.

TABLE XII. Adiabatic Electron Affinities, Comparisons between Theoretical and Experimental Values

molecule	HF[a,c]	CISD[a]	EM[a]	HFS[b,c]	LDA[b]	LDA/NL[b]	expt
CN	2.93	3.70	4.15	2.78	3.25	3.51	3.82[d]
BO	1.41	2.35	2.97	1.25	1.96	2.33	3.1[e] 2.2[f]
OCN	2.28	3.21	-	2.83	3.19	3.35	3.6[g]
N_3	0.89	2.15	-	2.12	2.50	2.65	2.7[h]
NO_2	1.51	2.00		1.02	1.43	1.90	2.32[i]

[a] Calculations[101] with extensive basis sets. [b] Calculations with basis set similar to that of ref 101. [c] Calculations on radical were unrestricted. [d] Berkowitz, J.; Chupka, W. A.; Walker, T. A. *J. Chem. Phys.* **1969**, *50*, 1497. [e] Srivastava, R. D.; Uy, W. A.; Farber, M. *Trans. Faraday Soc.* **1971**, *67*, 2941. [f] Gaines, A. F.; Page, F. M. *Trans. Faraday Soc.* **1966**, *62*, 3086. [g] Wight, C. A.; Beauchamp, J. L. *J. Phys. Chem.* **1980**, *84*, 2503. [h] Jackson, R. L.; Pellerite, M. J.; Brauman, J. I. *J. Am. Chem. Soc.* **1981**, *103*, 1802. [i] Woo, S. B.; Helmy, E. M.; Mauk, P. H.; Paszek, A. P. *Phys. Rev. A* **1981**, *24*, 1380.

The treatment of multiplets, avoided crossings, and weakly interacting systems within the framework of approximate DFT are still incomplete in spite of the progress described above. Much work remains to be done in this area which is emerging into one of the most challenging fields in approximate DFT.

H. Electron Affinity

Electron affinity, EA, plays, together with ionization energy, a key role in the theory of chemical reactivity developed by Parr[96] and Pearson. This theory, which is discussed by Parr,[6] is an extension of Pearsons[98] original concept of hardness and softness. The extension is based on DFT.

The adiabatic electron affinity, $\mathrm{EA}_{\mathrm{ad}}$, from the process

$$A + e^- \rightarrow A^- - \mathrm{EA}_{\mathrm{ad}} \qquad (26)$$

is difficult to evaluate theoretically for molecules. One has to evaluate the equilibrium geometries of A and A^- as well as the energy difference between A and A^- in their respective ground-state conformations. The calculation of molecular electron affinities by approximate DFT has been carried out extensively by Gutsev[99] et al. We compare in Table XII calculated $\mathrm{EA}_{\mathrm{ad}}$ values with experiment. The comparison includes[100] HFS, LDA, as well as LDA with nonlocal exchange corrections[23d] (LSD/NL). Also included are results[101] based on HF, configuration interaction with all single and doubles (RCISD), as well as the equation of motion approach[102] (EOM). Several experimental $\mathrm{EA}_{\mathrm{ad}}$ values have been published for each of the molecules in Table XII, covering quite a range. The experimental data selected represents what currently is considered to represent the best estimates. Flexible basis sets are crucial[101] in theoretical evaluations of $\mathrm{EA}_{\mathrm{ad}}$ and all calculations were carried out with extensive basis sets.

It follows from Table XII that HF and HFS, in which correlation between electrons of different spins are absent, underestimate $\mathrm{EA}_{\mathrm{ad}}$. This is understandable as the lack of correlation is more crucial (destabilizing) for the negative ions A^- than the neutral species. This is so since A^- has one more pair of electrons than A. Thus the exclusion of correlation will underestimate the energy gap between A and A^-. The explicit inclusion of electron correlation greatly improves the theoretical results both in the case of the ab initio methods (CISD, EOM) as well as in the case of the DFT-based LDA scheme. The addition of nonlocal exchange correction[23d] to LDA (LDA/NL) is seen further to bring the theoretical results in line with experiment. It seems clear that approximate DFT calculations on $\mathrm{EA}_{\mathrm{ad}}$ requires the inclusion of both electron correlation and nonlocal correction. However, at that level of approximate DFT the calculated results are comparable in quality to ab initio values based on extensive configuration interaction (CISD and EOM). Approximate DFT has also been used to calculate atomic electron affinities.

I. Miscellaneous

We shall finish our assessment by a brief discussion of DFT calculations on expectation values which primarily depend on the one-electron density, $\rho(\vec{r}_1)$, or the one-electron density matrix, $\rho(\vec{r}_1,\vec{r}_1{}')$. We will refer to these expectation values as one-electron properties.

The approximate Kohn–Sham equation (eq 15a) affords a set of one-electron orbitals $\{\tilde{\phi}_i(\vec{r}_1), i = 1, n\}$ from which one can calculate the approximate electron density as

$$\tilde{\rho}(\vec{r}_1) = \sum_{i=1}^{i=n} \tilde{\phi}_i(\vec{r}_1)\tilde{\phi}_i(\vec{r}_1) \qquad (27)$$

The approximate electron density $\tilde{\rho}(\vec{r}_1)$ will approach the exact density $\rho_{\mathrm{ex}}(\vec{r}_1)$ as $\tilde{V}_{\mathrm{XC}}[\rho(\vec{r}_1)]$ of eq 15d approaches the exact Kohn–Sham potential, V_{XC}. Thus the exact Kohn–Sham orbitals $\{\phi_i(\vec{r}_1), i = 1, n\}$ represent the optimal set of one-electron functions from which one can construct the one-electron density from eq 27. It is even possible, as we shall see shortly, that the approximate Kohn–Sham orbitals $\{\tilde{\phi}_i(\vec{r}_1), i = 1, n\}$ via eq 27 afford a density $\tilde{\rho}(\vec{r}_1)$ which is closer to $\rho_{\mathrm{ex}}(\vec{r}_1)$ than the HF density, $\rho^{\mathrm{HF}}(\vec{r}_1)$, given by $\rho^{\mathrm{HF}}(\vec{r}_1) = \sum_i^{\mathrm{HF}}(\vec{r}_1)\text{-}\phi_i^{\mathrm{HF}}(\vec{r}_1)$.

The one-electron density matrix, $\rho(\vec{r}_1,\vec{r}_1{}')$, is not readily obtained from (approximate) DFT. It is customary to make use of the approximate expression

$$\tilde{\rho}(\vec{r}_1,\vec{r}_1{}') = \sum_{i=1}^{i=n} \tilde{\phi}_i(\vec{r}_1)\tilde{\phi}_i(\vec{r}_{1'}) \qquad (28)$$

applicable for a single determinantal wave function constructed from the set of orbitals $\{\tilde{\phi}_i(\vec{r}_1), i = 1, n\}$. We note that $\tilde{\rho}(\vec{r}_1,\vec{r}_1{}')$ will differ from the exact one-electron density matrix even if $\{\tilde{\phi}_i(\vec{r}_1), i = 1, n\}$ represents the true set of Kohn–Sham orbitals. It is not clear a priori whether $\tilde{\rho}(\vec{r}_1,\vec{r}_1{}')$ constructed from approximate Kohn–Sham orbitals according to eq 28 will be more appropriate than the HF one-electron density matrix, $\tilde{\rho}_{\mathrm{HF}}(\vec{r}_1,\vec{r}_1{}') = \sum\phi_i^{\mathrm{HF}}(\vec{r}_1)\phi_i^{\mathrm{HF}}(\vec{r}_{1'})$.

There have been a number of DFT-based calculations on one-electron properties including parameters from NMR[103,104] and ESR[95c] spectroscopy, electric-field gradients[105] and other Mössbauer parameters,[106] dipole moments,[65,107] dipole moment derivatives,[65,107] UV intensities,[108] optical activity,[109] diamagnetic properties,[110] and polarizabilities.[107c,111]

It is not as yet clear from the many DFT-based calculations on one-electron properties whether the one-electron matrix $\tilde{\rho}(\vec{r}_1,\vec{r}_1{}')$ of eq 28, which is constructed from approximate Kohn–Sham orbitals, in fact is more adequate than $\tilde{\rho}_{\mathrm{HF}}(\vec{r}_1,\vec{r}_1{}')$ from ordinary HF theory. It seems, however, quite evident that the electron density

TABLE XIII. Calculated Dipole Moment (μ_z) and Polarizability (α_{xx}, α_{yy}, α_{zz}) of H_2O (All Units in Atomic Units)

	LDA^a	HF^b	CI^c	CEPA-1^d	expt^a
μ_z	0.721	0.787	0.785	0.723	0.728
α_{xx}	9.403	7.83	9.02	9.59	9.26
α_{yy}	10.15	9.10	9.84	9.81	10.01
α_{zz}	9.75	8.36	9.33	9.64	9.62

[a] Reference 107c. [b] Dyke, T. R.; Muenter, J. S. *J. Chem. Phys.* **1973**, *59*, 3125. [c] Kirchhoff, W. H.; Lide, D. R. *Natl. Stand. Ref. Data. Ser. Natl. Bur. Stand.* **1967**, 10. [d] Clough, S. A.; Beers, Y.; Klein, G. P.; Rothman, L. S. *J. Chem. Phys.* **1973**, *59*, 2254.

TABLE XIV. Calculated Dipole Moments in Debye

molecule	LDA^a	LDA/NL^a	HF^b	expt^b
CO	−0.174	−0.153	0.33	−0.11
CS	2.107	2.014	1.26	1.98
LiH	5.65	5.74	5.77	5.83
HF	1.86	1.80	1.98	1.82

[a] Fan, L.; Ziegler, T. to be submitted for publication. [b] Reference 62.

from approximate DFT (eq 27) in most cases is more adequate than the HF density, $\rho^{HF}(\vec{r}_1)$. Table XIII presents calculations[107c] on the dipole moment and polarizability of H_2O with extensive basis sets. It follows that LDA affords results in much better accord with experiment than HF. In fact, the LDA values agree as well with experiment as the CEPA-1 results in which electron correlation is taken into account by configuration interaction. Polarizabilities in close agreement with experiment have been obtained[111] from HFS calculations on a number of small molecules. Not much data is available on how nonlocal corrections influence the calculated electron density. The calculated dipole moments in Table XIV seem to indicate that the inclusion of nonlocal corrections to exchange[23d] and correlation[25] has a small but important influence on the calculated dipole moments.

Much work still needs to be done before it is possible to assess the quality of one-electron properties calculated by approximate DFT. It is, however, encouraging that dipole moments and polarizabilities are accurately represented. This would indicate that in addition to accurate vibrational frequencies one will also be able to calculate accurate IR and Raman intensities.

IV. Acknowledgment

I thank E. J. Baerends, J. G. Snijders, P. Vernooijs, and W. Ravenek (Free University of Amsterdam) as well A. D. Becke (Queens University, Canada) and D. E. Ellis (Northwestern University) for all the insight and assistance they have supplied over the past 15 years. I thank L. Fan, V. Tschinke, and L. Versluis (University of Calgary, Canada) for their contributions to the practical implementation and computational evaluation of approximate density functional theories and a special thanks to my former supervisor Arvi Rauk (University of Calgary) for his help. This investigation was supported by the Natural Sciences and Engineering Research Council of Canada (NSERC).

References

(1) (a) Dirac, P. A. M. *Cambridge Philos. Soc.* **1930**, *26*, 376. (b) Fermi, E. *Z. Phys.* **1928**, *48*, 73. (c) Thomas, L. H. *Proc. Cambridge Philos. Soc.* **1927**, *23*, 542. (d) Gombas, P. In *Die Statistischen Theorie des Atomes und Ihre Anwendungen*; Springer-Verlag: West Berlin, 1949. (e) March, N. H. *Adv. Phys.* **1957**, *6*, 1. (f) March, N. H. *Self-Consistent Fields in Atoms*; Pergamon: Oxford, 1975. (g) Wigner, E. P. *Phys. Rev.* **1934**, *46*, 1002.

(2) (a) Slater, J. C. *Phys. Rev.* **1951**, *81*, 385. (b) Gáspár *Acta Phys. Acad. Sci. Hung.* **1954**, *3*, 263. (c) Slater, J. C. *Adv. Quantum. Chem.* **1972**, *6*, 1. (d) Slater, J. C. *The self-Consistent Field for Molecules and Solids: Quantum Theory of Molecules and Solids*; McGraw Hill: New York, 1974; Vol. 4.

(3) (a) Hohenberg, P.; Kohn, W. *Phys. Rev. A* **1964**, *136*, 864. (b) Levy, M. *Proc. Natl. Acad. Sci. U.S.A.* **1979**, *76*, 6062.

(4) (a) Kohn, W.; Sham, L. J. *Phys. Rev. A* **1965**, *140*, 1133. (b) Kohn, W.; Vashishta, P. In ref 8b, pp 79–147.

(5) (a) Dahl, J. P., Avery, J., Eds. *Local Density Approximations in Quantum Chemistry and Solid-State Physics*; Plenum: New York, 1984. (b) Dreizler, R. M., da Providencia, J., Eds. *Density Methods in Physics*; Plenum: New York, 1985. (c) Erdahl, R., Smith, V. H., Eds. *Density Matrices and Density Functionals*; Reidel: Dordrecht, 1987. (e) Keller, J., Gázquez, J. L., Eds. *Density Functional Theory*. Lecture Notes in Physics 187, Springer: Heidelberg, 1983.

(6) (a) Parr, R. G.; Yang, W. *Density-Functional Theory of Atoms and Molecules*; Oxford University Press: New York, 1989. (b) Kryachko, E. S.; Ludena, E. V. *Density Functional Theory of Many Electron Systems*; Kluwer Press: Dordrecht, in press. (c) March, N. H. *Electron Density Theory of Atoms and Molecules*; Academic Press: New York, in press. (d) Sham, L. J.; Schlüter, M., Eds. *Principles and Applications of Density Functional Theory*; Teanec, in press.

(7) (a) Parr, R. G. *Ann. Rev. Phys. Chem.* **1983**, *34*, 631. (b) Borman, S. *Chem. Eng. News* **1990**, *68*(15), 22.

(8) (a) Callaway, J.; March, N. H. *Solid State Phys.* **1984**, *38*, 135. (b) Lundqvist, S., March, N. H., Eds. *Theory of the Inhomogeneous Electron Gas*; Plenum: New York, 1984. (c) Langreth, D., Suhl, H., Eds. *Many-Body Phenomena at Surfaces*, Academic Press: Orlando, 1983.

(9) (a) Jones, R. O. *Adv. Chem. Phys.* **1987**, *67*, 413.

(10) (a) Connolly, J. W. D. *Semiempirical Methods of Electronic Structure Calculations, Part A: Techniques.*; Segal, G. A., Ed.; Plenum: New York, 1977. (b) Case, D. A. *Annu. Rev. Phys. Chem.* **1982**, *33*, 151.

(11) (a) A clear discussion of this point can be found in ref 11b. (b) Becke, A. D. *J. Chem. Phys.* 1988, *88*, 1053. (c) Becke, A. D. *ACS Symp. Ser.* **1989**, *394*.

(12) (a) McWeeney, R.; Sutcliffe, B. T. *Methods of Molecular Quantum Mechanics*; Academic Press: New York, 1969. (b) Luken, W. L.; Beratan, D. N. *Theoret. Chim. Acta.* **1982**, *61*, 265.

(13) (a) Gunnarsson, O.; Lundquist, I. *Phys. Rev.* **1974**, *B10*, 1319. (b) Gunnarsson, O.; Lundquist, I. *Phys. Rev.* **1976**, *B13*, 4274. (c) Gunnarsson, O.; Johnson, M.; Lundquist, I. *Phys. Rev.* **1979**, *B20*, 3136.

(14) (a) It is possible to find V_{XC} for two electronic systems to a very high accuracy as discussed in ref 14b. (b) Buijse, M.; Baerends, E. J.; Snijders, J. G. *Phys. Rev.* **1989**, *A40*, 4190.

(15) von Barth, U.; Hedin, L. *Phys. Rev.* **1979**, *A20*, 1693.

(16) Vosko, S. J.; Wilk, L.; Nusair, M. *Can. J. Phys.* **1980**, *58*, 1200.

(17) Ceperley, D. M.; Alder, B. J. *Phys. Rev. Lett.* **1980**, *45*, 566.

(18) (a) Schwarz, K. *Phys. Rev.* **1972**, *B5*, 2466. (b) Gopinathan, M. S.; Whitehead, M. A. *Phys. Rev.* **1976**, *A14*, 1.

(19) Tschinke, V.; Ziegler, T. *Can. J. Chem.* **1989**, *67*, 460.

(20) Becke, A. D. *Int. J. Quantum Chem.* **1983**, *23*, 1915.

(21) Perdew, J. P. *Phys. Rev. Lett.* **1985**, *55*, 1665.

(22) Herman, J. P., Van Dyek, J. P. *Phys. Rev. Lett.* **1969**, *22*, 807.

(23) (a) Perdew, J. P.; Wang, Y. *Phys. Rev.* **1986**, *B33*, 8800. Perdew, J. P.; Wang, Y. *Phys. Rev.* **1989**, *40*, 3399 (erratum). (b) Langreth, D. C.; Mehl, M. J. *Phys. Rev.* **1983**, *B29*, 2310. (c) Becke, A. D. *Phys. Rev.* **1986**, *A33*, 2786. (d) Becke, A. D. *Phys. Rev.* 1988, *A38*, 2398. (e) DePristo, A. E.; Kress, J. D. *J. Chem. Phys.* **1987**, *86*, 142.

(24) Stoll, H.; Golka, E.; Preuss, H. *Theor. Chim. Acta.* **1978**, *49*, 143.

(25) Perdew, J. P. *Phys. Rev.* **1986**, *B33*, 8822. Perdew, J. P. *Phys. Rev.* **1986**, *B34*, 7406 (erratum).

(26) (a) Lee, C.; Yang, W.; Parr, R. G. *THEOCHEM* **1987**, *163*, 305. (b) Colle, R.; Salvetti, O. *Theor. Chim. Acta.* **1975**, *37*, 329. (c) Levy, M. *Int. J. Quantum Chem.* **1989**, *S23*, 617.

(27) (a) Savin, A.; Stoll, H.; Preuss, H. *Theor. Chim. Acta.* **1986**, *70*, 407. (b) Savin, A.; Wedig, V.; Preuss, H.; Stoll, H. *Phys. Rev. Lett.* **1984**, *53*, 2087.

(28) Jones, R. O. *Phys. Rev. Lett.* **1985**, *55*, 107.

(29) (a) Tschinke, V.; Ph.D. Thesis, University of Calgary, 1989. (b) Tschinke, V.; Ziegler, T. *J. Chem. Phys.* **1990**, *93*, 8051. (c) Tschinke, V.; Ziegler, T. *Theor. Chim. Acta*, submitted for publication. (d) Tschinke, V.; Ziegler, T. ref 5c, p 467.

(30) Kemister, G.; Nordholm, S. *J. Chem. Phys.* **1985**, *83*, 5163.

(31) (a) For a clear discussion of the difference between dynamic correlation and near degeneracy correlation see ref 31b. (b) McWeeny, R. In: *The New World of Quantum Chemistry*; Pullman, B., Parr, R., Eds.; D. Reidel: Dordrecht, 1976.

(32) Cook, M.; Karplus, M. *J. Phys. Chem.* **1987**, *91*, 31.

(33) (a) Lie, G. C.; Clementi, E. *J. Chem. Phys.* **1974**, *60*, 1275. (b) Chakravorty, S.; Clementi, E. *Phys. Rev. A*, **1989**, *39*, 2290. (c) Savin, A.; Stoll, H.; Preuss, H. *Theor. Chim. Acta.* **1986**, *70*, 407. (d) Roos, B. O.; Szulkin, M.; Jaszunski, M. *Theor. Chim. Acta.* **1987**, *71*, 375.

(34) (a) For a general review of this approach see ref 34b. (b) Clementi, E.; Chakravorty, S. J.; Corongiu, G.; Carravetta, V. In *Modern Techniques in Computational Chemistry*; Clementi, E., Ed.; Escom: Leiden, 1989.

(35) Krishna, M. V. R. *J. Comp. Chem.* **1990**, *11*, 629.

(36) Savin, A. *Int. J. Quant. Chem.* **1988**, *S22.*

(37) Johnson, K. H. *J. Chem. Phys.* **1966**, *45*, 3085.

(38) Korringa, J. *Physica* **1947**, *13*, 392.

(39) Salahub, D. R.; Messmer, R. P.; Johnson, K. H. *Mol. Phys.* **1976**, *31*, 521.

(40) Ellis, D. E.; Painter, G. S. *Phys. Rev.* **1970**, *B2*, 2887.

(41) Baerends, E. J.; Ellis, D. E.; Ros, P. *Chem. Phys.* **1973**, *2*, 41.

(42) Sambe, H.; Felton, R. H. *J. Chem. Phys.* **1975**, *62*, 1122.

(43) (a) Dunlap, B. I.; Connolly, J. W. D.; Sabin, J. F. *J. Chem. Phys.* **1979**, *71*, 4993. (b) Dunlap, B. I.; Connolly, J. W. D.; Sabin, J. F. *J. Chem. Phys.* **1983**, *78*, 4787.

(44) Gunnarson, O.; Harris, J.; Jones, R. O. *Phys. Rev.* **1977**, *15*, 3027.

(45) (a) Delley, B.; Ellis, D. E. *J. Chem. Phys.* **1982**, *76*, 1949. (b) Gutsev, G. L.; Levin, A. A. *Chem. Phys.* **1980**, *51*, 459. (c) Bieger, W.; Seifert, G.; Grossmann, G. *Z. Chem.* **1984**, *24*, 156. (d) Kutzler, F. W.; Painter, G. S. *Phys. Rev. B* **1988**, *37*, 285. (e) Pederson, M. A.; Klein, B. M.; Broughton, J. Q. *Phys. Rev. B* **1988**, *38*, 3825.

(46) (a) Becke, A. D. *J. Chem. Phys.* **1988**, *88*, 2547. (b) Boerrigter, P. M.; te Velde, G.; Baerends, E. J. *Int. J. Quantum Chem.* **1988**, *33*, 87. (c) Delley, B. *J. Chem. Phys.* **1990**, *92*, 508. (d) te Velde, G.; Baerends, E. J. *J. Comp. Phys.*, submitted for publication. (e) Pederson, M. R.; Jackson, K. A. *Phys. Rev. B* **1990**, *41*, 7453.

(47) (a) Ravenek, W. In *Algorithms and Applications on Vector and Parallel Computers*; the Riele, H. J. J., Dekker, T. J., van de Vorst, H. A., Eds.; Elsevier: Amsterdam, 1987. (b) Ravenek, W. In *Scientific Computing on Supercomputers*; de Vreese, J., van Camp, P. E., Eds.; Plenum: New York, 1989. (c) The LCAO-HFS program will be available from Polygen.

(48) (a) Wimmer, E.; Freeman, A.; Fu, C.-L.; Cao, S.-H.; Delley, B. In *Supercomputer Research in Chemistry and Chemical Engineering*; Jensen, K. F., Truhlar, D. G., Eds.; ACS Symposium Series 353; American Chemical Society: Washington, DC, 1987; p 49. (b) Andzelm, J.; Wimmer, E.; Salahub, D. R. In *Spin Density Functional Approach to the Chemistry of Transition Metal Clusters*; Salahub, D. R., Zerner, M. C., Eds. ACS Symposium Series 394, American Chemical Society: Washington, DC, 1989; p 229. (c) DGauss available from CRAY. (d) DMol available from Biosym. (e) DMon is developed by Salahub et al. at University of Montreal, Canada. (f) NUMOL is developed by Becke at Queens University, Kingston, Canada.

(49) Ziegler, T.; Rauk, A. *Theor. Chim. Acta.* **1977**, *46*, 1.

(50) (a) Becke, A. D. *J. Chem. Phys.* **1982**, *76*, 6037. (b) Becke, A. D. *J. Chem. Phys.* **1983**, *78*, 4787. (c) Becke, A. D.; Dickson, R. M. *J. Chem. Phys.* **1988**, *89*, 2993. (d) Becke, A. D. *Int. J. Quantum Chem.* **1989**, *S23*, 599. (e) Becke, A. D.; Dickson, R. M. *J. Chem. Phys.* **1990**, *92*, 3610. (f) The program outlined in ref 50d–e is called NUMOL.

(51) (a) Laaksonen, L.; Sundholm, D.; Pyykkö, P. *Comput. Phys. Rept.* **1986**, *4*, 313. (b) Heinemann, D.; Fricke, B.; Kolb, D. *Phys. Rev.* **1988**, *A38*, 4998. (c) Heinemann, D.; Rosén; Fricke, B. *Chem. Phys. Lett.* **1990**, *166*, 627.

(52) (a) Snijders, J. G.; Baerends, E. J. *Mol. Phys.* **1977**, *33*, 1651. (b) Andzelm, J.; Radzio, E.; Salahub, D. R. *J. Chem. Phys.* **1985**, *83*, 4573. (c) Ravenek, W., Ph.D. Thesis, Nijmegen, 1983. (d) Ravenek, W.; Baerends, E. J. *J. Chem. Phys.* **1984**, *81*, 865.

(53) (a) Snijders, J. G.; Baerends, E. J. *Mol. Phys.* **1978**, *36*, 1789. (b) Snijders, J. G.; Baerends, E. J.; Ros, P. *Mol. Phys.* **1979**, *38*, 1909. (c) Gollisch, H.; Fritsche, L. *Phys. Status. Solidi* **1978**, *B86*, 145. (d) Koelling, D. D.; Harmon, P. N. *J. Phys.* **1977**, *C10*, 3107. (e) Ellis, D. E.; Rosen, A. *Z. Phys.* **1977**, *A283*, 3. (f) Yang, C. Y.; Rabii, S. *Phys. Rev.* **1975**, *A12*, 362.

(54) (a) Satoko, C. *Chem. Phys. Lett.* **1981**, *83*, 111. (b) Fournier, R.; Andzelm, J.; Salahub, D. R. *J. Chem. Phys.* **1989**, *90*, 6371. (c) Versluis, L.; Ziegler, T. *J. Chem. Phys.* **1988**, *88*, 322. (d) Averill, F. W.; Painter, G. S. *Phys. Rev.* **1985**, *B32*, 2141. (e) Satoko, C. *Phys. Rev.* **1984**, *30*, 1754. (f) Harris, J.; Jones, R. O.; Mueller, J. E. *J. Chem. Phys.* **1981**, *75*, 3904. (g) Martins, L.; Buttet, J.; Car, R. *Phys. Rev. Lett.* **1984**, *53*, 655. (h) Jackson, K.; Pederson, M. R. *Phys. Rev. B* **1990**, in press.

(55) Buijse, M.; Baerends, E. J. *J. Chem. Phys.* **1990**, *93*, 4129.

(56) Ziegler, T.; Tschinke, V.; Ursenbach, C. *J. Am. Chem. Soc.* **1987**, *109*, 4825.

(57) (a) Ziegler, T. In ref 5a, p 273. (b) Ziegler, T.; Rauk, A.; Baerends, E. J. *Theor. Chim. Acta* **1977**, *43*, 261. (c) von Barth, U. *Phys. Rev.* **1979**, *20*, 1693. (d) Gunnarsson, O.; Jones, R. O. *Phys. Scr.* **1980**, *21*, 394.

(58) Ziegler, T.; Tschinke, V.; Ursenbach, C. *J. Am. Chem. Soc.* **1987**, *109*, 4825.

(59) Ziegler, T.; Tschinke, V.; Becke, A. *Polyhedron* **1987**, *6*, 685.

(60) Ziegler, T.; Tschinke, V.; Becke, A. *J. Am. Chem. Soc.* **1987**, *109*, 1351. (b) Ziegler, T.; Cheng, W.; Baerends, E. J.; Ravenek, W. *Inorg. Chem.* **1988**, *27*, 3458. (c) Ziegler, T.; Tschinke, V.; Baerends, E. J.; Snijdes, J. G.; Ravenek, W. *J. Phys. Chem.* **1989**, *93*, 3050. (d) Ziegler, T.; Snijders, J. G.; Baerends, E. J. *J. Chem. Phys.* **1981**, *74*, 5737.

(61) Ziegler, T.; Tschenke, V.; Versluis, L.; Baerends, E. J.; Ravenek, W. *Polyhedron* **1988**, *7*, 1625.

(62) Hehre, W. J.; Radom, L.; Schleyer, P. v. R.; Pople, J. A. In *Ab initio Molecular Theory*; Wiley: New York, 1986.

(63) (a) Moccia, R. *Theor. Chim. Acta.* **1967**, 8, 8. (b) Fletcher, R. *Mol. Phys.* **1970**, *19*, 55. (c) McIver, J. W.; Kormonicki, A. *Chem. Phys. Lett.* **1971**, *10*, 303. (d) Pulay, P. *Chem. Phys. Lett.* **1969**, *17*, 197. (e) Pople, J. A.; Krishnan, R.; Schlegel, H. B.; Binkley, J. S. *Int. J. Quantum Chem.* **1979**, *S13*, 225.

(64) (a) Lüthi, H. P.; Siegbahn, P. E. M.; Almlöf, J. *J. Phys. Chem.* **1985**, *89*, 2156. (b) Lüthi, H. P.; Ammeter, J. A.; Almlöf, J.; Faegri, K. *J. Chem. Phys.* **1982**, *77*, 2002. (c) Antolovic, D.; Davidson, E. R. *J. Chem. Phys.* **1988**, *88*, 4967.

(65) Baerends, E. J.; Ros, P. *Int. J. Quantum Chem.* **1978**, *S12*, 169.

(66) (a) Rösch, N.; Jorg, H.; Dunlap, B. I. *NATO ASI* **1985**, *176*, 179. (b) Dunlap, B. I. *J. Phys. Chem.* **1986**, *90*, 5524. (c) Versluis, L.; Ziegler, T. *J. Am. Chem. Soc.* **1989**, *111*, 2018.

(67) Labanowski, J., Andzelm, J., Eds. *Density Functional Methods in Chemistry*; Springer-Verlag: Heidelberg, 1991.

(68) (a) Delley, B.; Freeman, A. J.; Ellis, D. E. *Phys. Rev. Lett.* **1983**, *50*, 488. (b) Chou, S. H.; Freeman, A. J.; Grigoras, S.; Gentle, T. M.; Delley, B.; Wimmer, E. *J. Am. Chem. Soc.* **1987**, *109*, 1987. (c) Freeman, A. J.; Ellis, D. E.; Delley, B. *Phys. Rev. B* **1989**, *40*, 6277. (d) Ling, Y.; Freeman, A. J.; Delley, B. *Phys. Rev.* **1989**, *B39*, 10144.

(69) (a) Andzelm, J. W. ref 67, p 155 and p 411. (b) Pederson, M. R.; Jackson, K. A. ref 67, p 247. (c) Dixon, D. A. ref 67, p 33. (d) Salahub, D. R. ref 67, p 77. (e) Delley, B. ref 67, p 61; p 101. (f) Teter, M. ref 67.

(70) (a) Ziegler, T. *J. Am. Chem. Soc.* **1983**, *105*, 7543. (b) Ziegler, T. *J. Am. Chem. Soc.* **1984**, *106*, 5901. (c) Ziegler, T. *J. Am. Chem. Soc.* **1985**, *107*, 4453. (d) Ziegler, T.; Tschinke, V.; Becke, A. *Polyhedron* **1986**, *6*, 685.

(71) (a) van der Knaap, T. A.; Bickelhaupt, F.; Kraaykamp, J. G.; van Koten, G.; Bernards, J. C. P.; Edzes, H. T.; Weeman, W. S.; de Boer, E.; Baerends, E. J. *Organometallics* **1984**, *3*, 1804. (b) Bickelhaupt, F. M.; Baerends, E. J.; Ravenek, W. *Inorg. Chem.* **1990**, *29*, 350. (c) Ziegler, T.; Rauk, A. *Inorg. Chem.* **1979**, *18*, 1558. (d) Ziegler, T. *Inorg. Chem.* **1985**, *24*, 1547. (e) Hitchcock, A. P.; Hao, N. G.; Werstiuk, N. H.; McGlinchey, M. G.; Ziegler, T. *Inorg. Chem.* **1982**, *21*, 793. (f) Ziegler, T. *Inorg. Chem.* **1986**, *25*, 2723. (g) DeKock, R. L.; Baerends, E. J.; Hengelmolen, R. *Organometallics* **1984**, *3*, 289. (h) Ziegler, T. *Organometallics* **1985**, *4*, 675. (i) Famiglietti, C.; Baerends, E. J. *Chem. Phys.* **1981**, *62*, 407.

(72) (a) Ziegler, T. *NATO ASI* **1985**, 176. (b) Ziegler, T.; Rauk, A. *Inorg. Chem.* **1979**, *18*, 1755.

(73) (a) Caffarel, M.; Claverie, P.; Mijoule, C.; Andzelm, J.; Salahub, D. R. *J. Chem. Phys.* **1989**, *90*, 990. (b) Selmani, A.; Andzelm, J.; Salahub, D. R. *Int. J. Quantum Chem.* **1986**, *14*, 829. (c) Andzelm, J.; Salahub, D. R. *Int. J. Quantum Chem.* **1986**, *14*, 1091. (d) Baykara, N. A.; Andzelm, J.; Salahub, D. R.; Baykara, S. Z. *Int. J. Quantum Chem.* **1986**, *14*, 1025. (e) Baycara, N. A.; McMaster, B. N.; Salahub, D. R. *Mol. Phys.* **1984**, *52*, 891.

(74) (a) Rösch, N.; Knappe, P.; Sandl, P.; Görling, A.; Dunlamp, B. L. *ACS Symposium Ser.* **1989**, *394*, 180, and references cited therein.

(75) (a) Dunlap, B. I. *Phys. Rev. A* **1990**, *41*, 5691. (b) Mintmire, J. W.; Dunlap, B. I.; Brenner, D. W.; Mowrey, R. C.; Ladouceur, H. D.; Schmidt, P. P.; White, C. T.; O'Grady, W. E. *Phys. Lett.* **1989**, *A138*, 51. (c) Rösch, N.; Sandl, P.; Knappe, P.; Görling, A.; Dunlap, B. I. *Z. Phys.* **1989**, *D12*, 547.

(76) (a) Post, D.; Baerends, E. J. *Surface Sci.* **1981**, *109*, 167. (b) Post, D.; Baerends, E. J. *Chem. Phys. Lett.* **1982**, *86*, 176. (c) Post, D.; Baerends, E. J. *Surface Sci.* **1982**, *116*, 177. (d) Delley, B.; Ellis, D. E.; Freeman, A. J.; Baerends, E. J.; Post, D. *Phys. Rev.* **1983**, *B27*, 5663. (e) Post, D.; Baerends, E. J. *J. Chem. Phys.* **1983**, *78*, 5663. (f) Ravenek, W.; Jansen, A. P. J.; van Santen, R. A. *J. Phys. Chem.* **1989**, *93*, 6445. (g) van den Hoek, P. J.; Baerends, E. J.; van Santen, R. A. *J.*

Phys. Chem. **1989**, *93*, 6469. (h) Ravenek, W.; Geurts, M. M. *J. Chem. Phys.* **1986**, *84*, 1613.

(77) (a) Spruit, M. E. M.; van den Hoek, P. J.; Kuipers, E. W.; Geuzebroek, F. H.; Kleyn, A. W. *Surface Sci.* **1989**, *214*, 591. (b) van den Hoek, P. J.; Kleyn, A. W.; Baerends, E. J. *Mol. Phys.* **1989**, *23*, 93.

(78) (a) van den Hoek, P. J. Ph.D. Thesis, The Free University, Amsterdam, 1989. (b) van den Hoek, P. J.; Ravenek, W.; Baerends, E. J. *Phys. Rev. Lett.* **1988**, *60*, 1743. (c) van den Hoek, P. J.; Ravenek, W.; Baerends, E. J. *Phys. Rev.* **1988**, *B38*, 508. (d) van den Hoek, P. J.; Ravenek, W.; Baerends, E. J. *Surface Sci.* **1988**, *205*, 549.

(79) (a) Mintmire, J. W.; White, C. T. *Int. J. Quantum Chem.* **1987**, *S21*, 131. (b) Ortiz, J. V.; Mintmire, J. W. *J. Am. Chem. Soc.* **1988**, *110*, 4522. (c) Springborg, M.; Drechsler, S. F.; Malek, J. *Phys. Rev.* **1990**, *B41*, 11956. (d) Ashkenazi, J.; Pickett, W. E.; Klein, B. M.; Krakauer, H.; Wang, C. W. *Synth. Met.* **1987**, *21*, 301.

(80) Fan, L.; Ziegler, T. *J. Chem. Phys.* **1990**, *92*, 3645.

(81) Schneider, F. W.; Rabinovitch, B. S. *J. Am. Chem. Soc.* **1962**, *84*, 4215.

(82) Redom, L. T.; Purvis, G. D.; Bartlett, R. J. *J. Chem. Phys.* **1978**, *69*, 5386.

(83) (a) Peluso, A.; Salahub, D. R.; Goursot, A. *Inorg. Chem.* **1990**, *29*, 1544. (b) Harrod, J. F.; Ziegler, T.; Tschinke, V. *Organometallics* **1990**, *9*, 897. (c) Masters, A. P.; Sørensen, T. S.; Ziegler, T. *Organometallics* **1989**, *8*, 611. (d) Versluis, L.; Ziegler, T. *J. Am. Chem. Soc.* **1990**, *112*, 6763. (e) Versluis, L.; Ziegler, T. *Organometallics* **1990**, *9*, 2985. (f) Versluis, L.; Ziegler, T. *Inorg. Chem.* **1990**, *29*, 4530. (g) Ziegler, T.; Versluis, L.; Tschinke, V. *J. Am. Chem. Soc.* **1986**, *108*, 612. (h) Roe, D. C. *Organometallics* **1987**, *6*, 942. (i) Stoudland, P. O.; Bergman, R. G.; Noland, S. P.; Hoff, C. D. *Polyhedron* **1988**, *7*, 1429.

(84) Pulay, P. *Mol. Phys.* **1969**, *17*, 197.

(85) (a) Fan, L.; Versluis, L.; Ziegler, T.; Baerends, E. J.; Ravenek, W. *Int. J. Quantum Chem.* **1988**, *S22*, 173. (b) Papai, I.; St-Amant, A.; Fournier, R.; Salahub, D. R. *Int. J. Quantum Chem.* **1989**, *S23*.

(86) Fournier, R. *J. Chem. Phys.* **1990**, *92*, 5422.

(87) Baerends, E. J.; Snijders, J. G.; de Lange, C. A.; Jonkers, G. ref 5a., p 415.

(88) (a) Boerrigter, P. M., Ph.D. Thesis, The Free University, Amsterdam, 1987. (b) Boerrigter, P. M.; Baerends, E. J.; Snijders, J. G. *Chem. Phys.* **1988**, *122*, 357. (c) Boerrigter, P. M.; Snijders, J. G.; Dyke, J. M. *J. Electron Spectr. Rel. Phen.* **1988**, *46*, 43. (d) DeKock, R. L.; Baerends, E. J.; Boerrigter, P. M.; Hengelmolen, R. *J. Am. Chem. Soc.* **1984**, *106*, 3387.

(89) Noodleman, L.; Post, D.; Baerends, E. J. *Chem. Phys.* **1982**, *64*, 159.

(90) Bagus, P. S.; Bennett, B. I. *Int. J. Quantum Chem.* **1975**, *9*, 143.

(91) Von Barth, U. *Phys. Rev.* **1979**, *A20*, 1693.

(92) Gunnarsson, O.; Jones, R. O. *Physica Sc.* **1980**, *21*, 394.

(93) Dunlap, B. I. *Chem. Phys.* **1988**, *125*, 98.

(94) (a) Dunlap, B. I. *Adv. Chem. Phys.* **1987**, *69*, 287. (b) Dunlap, B. I. *Phys. Rev.* 1984, *A29*, 2902.

(95) (a) Noodleman, L.; Norman, J. G. *J. Chem. Phys.* **1979**, *70*, 4803. (b) Noodleman, L. *J. Chem. Phys.* **1981**, *74*, 5737. (c) Noodleman, L.; Baerends, E. J. *J. Am. Chem. Soc.* **1984**, *106*, 2316. (d) Noodleman, L.; Norman, J. G.; Osborne, J. H.; Aizman, A.; Case, D. A. *J. Am. Chem. Soc.* **1985**, *107*, 3418.

(96) Parr, R. G.; Pearson, R. G. *J. Am. Chem. Soc.* **1983**, *105*, 7512.

(97) Reference deleted in revision.

(98) (a) Pearson, R. G. *J. Am. Chem. Soc.* **1963**, *85*, 3533. (b) Pearson, R. G. *Inorg. Chem.* **1988**, *27*, 734.

(99) (a) Gutsev, G. L.; Boldyrev, A. I. *J. Phys. Chem.* **1990**, *94*, 2256. (b) Gutsev, G. L.; Boldyrev, A. I. *Russ. Chem. Rev.* **1987**, *56*, 519.

(100) Gutsev, G. L.; Ziegler, T. *J. Comp. Chem.*, submitted for publication.

(101) Baker, J.; Nobes, R. H.; Radom, L. *J. Comp. Chem.* **1986**, *3*, 349.

(102) Chen, T. T.; Smith, W. D.; Simons, J. *Chem. Phys. Lett.* **1974**, *26*, 296.

(103) (a) Bieger, W.; Seifert, G.; Eschrig, H.; Grossman, G. *Chem. Phys. Lett.* **1985**, *115*, 275. (b) Freier, D. A.; Fenske, R. F.; Xiao-Zeng, Y. *J. Chem. Phys.* **1985**, *83*, 3526. (c) Malkin, V. G.; Zhidomirov, Zh. *Strukt. Khim.* **1988**, *29*, 32.

(104) (a) van der Est, A. J.; Barker, P. B.; Burnell, E. E.; de Lange, C. A.; Snijders, J. G. *Mol. Phys.* **1985**, *56*, 161.

(105) (a) Ellis, D. E.; Guenzberger, D.; Jansen, H. B. *Phys. Rev.* **1983**, *B28*, 3697. (b) Snijders, J. G.; van der Meer, W.; Baerends, E. J.; de Lange, C. A. *J. Chem. Phys.* **1983**, *79*, 2970.

(106) Ravenek, W.; Jacobs, J. W. M.; van der Avoird, A. *Chem. Phys.* **1983**, *78*, 391.

(107) (a) Krijn, M. P. C. M., Ph.D. Thesis, Twente University, The Netherlands, 1988. (b) Baerends, E. J.; Vernooijs, P.; Rozendaal, A.; Boerrigter, P. M.; Krijn, M.; Feil, D.; Sundholm, D. *J. Mol. Struc. (THEOCHEM)* **1985**, *133*, 147. (c) Krijn, M. P. C. M.; Feil, D. *J. Chem. Phys.* **1987**, *91*, 540.

(108) (a) Noodleman, L. *J. Chem. Phys.* **1976**, *64*, 2343. (b) Ziegler, T.; Rauk, A.; Baerends, E. J. *Chem. Phys.* **1976**, *16*, 290.

(109) Rauk, A.; Barriel, J. M.; Ziegler, T. In *Progress in Theoretical Organic Chemistry*; Csizmadia, I. G., Ed.; Elsevier: Amsterdam, 1977; Vol. 2.

(110) Ravenek, W.; Geurts, F. M. M. *Chem. Phys.* **1984**, *81*, 865.

(111) Trsic, M.; Ziegler, T.; Laidlaw, W. G. *Chem. Phys.* **1976**, *15*, 383.